Long-term behaviour of Cs-137, Cs-133 and K in beech trees of French forests

Dina Okhrimchuk, Pierre Hurtevent, Marc Andre Gonze, Marie Simon-Cornu, Marine Roulier, Loic Carasco, Daniel Orjollet, Manuel Nicolas, Anne Probst

Journal of Environmental Radioactivity 277 (2024) 107450

Contents lists available at ScienceDirect

Journal of Environmental Radioactivity

journal homepage: www.elsevier.com/locate/jenvrad

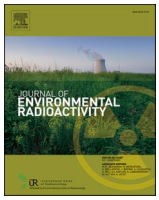

Long-term behaviour of Cs-137, Cs-133 and K in beech trees of French forests

D. Okhrimchuk [a], P. Hurtevent [a,*], M.-A. Gonze [a], M. Simon-Cornu [a], M. Roulier [a], L. Carasco [a], D. Orjollet [a], M. Nicolas [b], A. Probst [c]

[a] Institut de Radioprotection et de Sûreté Nucléaire (IRSN), PSE-ENV/SERPEN/LEREN, PSE-ENV/SPDR/LT2S, PSE-ENV/STAAR/LRTA, F-13115 Saint-Paul-lez-Durance, France

[b] ONF/Département Recherche-Développement-Innovation, F-77330, Fontainebleau, France

[c] CRBE (Centre de Recherche sur la Biodiversité et l'Environnement), Université de Toulouse, CNRS, IRD, Toulouse INP, Université Toulouse 3 – Paul Sabatier (UT3), F-31062, Toulouse, France

ARTICLE INFO

Keywords:
Cs-137
Cs-133
Long-term distribution
French forests
Beeches
Root transfer

ABSTRACT

In the long-term after atmospheric deposit onto a forest ecosystem, Cs-137 becomes incorporated into the biogeochemical cycle of stable elements and progressively reaches a quasi-equilibrium state. This study aimed at determining to what extent Cs-137 activity distribution in tree vegetation could be predicted from that of stable caesium (Cs-133) and potassium (K), which are known to be stable chemical analogues and competitors for Cs-137 intake in tree organs. Field campaigns that focused on beech trees (Fagus sylvatica L.) were conducted in 2021 in three French forest stands with contrasted characteristics regarding either the contribution of global vs. Chornobyl fallouts, soil or climatic conditions. Decades after Cs-137 fallouts, it was found that more than 80% of the total radioactive inventory in the system remained confined in the top 20 cm mineral layers, while organic layers and beech vegetation (including roots) contributed each to less than 1.5%. The enhanced downward migration of Cs-137 in cambisol than podzol forest sites was presumably due to migration of clay particles and bioturbation. The distribution of Cs-137 and Cs-133 inventories in beech trees was very similar among sites but differed from that of K due a higher accumulation of Cs isotopes in roots (40–50% vs. $<$ 25% for K). The aggregated transfer factor (*Tag*) of Cs-137 calculated for aerial beech organs were all lower than those reported in literature more than 20 years ago, this suggesting a decrease of bioavailability in soil due to ageing processes. Regarding their variability, *Tag*s were generally lower by a factor 5 at the cambisol site, which was fairly well explained by a much higher value of *RIP* (radiocesium immobilisation potential). Cs-137 concentrations in trees organs normalized by the soil exchangeable fractions were linearly correlated to those of Cs-133 and the best fit was found for the linear regression model without intercept indicating that no more contribution of the foliar uptake could be observed on long term. Provided that the vertical distribution of caesium concentrations and fine root density are properly measured or estimated, Cs-133 was shown to be a much better proxy than K to estimate the root transfer of Cs-137.

1. Introduction

In case of a severe nuclear accident (Chornobyl, Fukushima), caesium radioisotopes are likely to be released into the atmosphere in large quantities and deposited onto the ground surfaces (Steinhauser et al., 2014). Due to its long half-life (30.2 years), Cs-137 will rapidly become one of the main lasting contributors to the radioactivity content remaining in soil and perennial vegetation of the contaminated territories, with a long-term radiological impact on humans and biota. Forests are particularly sensitive ecosystems because they are very efficient at intercepting gaseous or particulate radionuclides, and are capable of retaining them in their soils and their internal biogeochemical cycling process over decades (e.g. Tikhomirov et al., 1993; Tikhomirov and Shcheglov, 1994). Following atmospheric testing of nuclear bombs (from the mid-1940s to the mid-1980s) or nuclear accidents such as Chornobyl (April 1986) and Fukushima (March 2011), high contamination levels of radiocaesium often persisted for years or decades in forest foodstuffs such as mushrooms or game as well as in wood

* Corresponding author.
E-mail address: pierre.hurtevent@irsn.fr (P. Hurtevent).

https://doi.org/10.1016/j.jenvrad.2024.107450
Received 29 January 2024; Received in revised form 4 April 2024; Accepted 12 May 2024
Available online 18 May 2024

products (Calmon et al., 2009). Forest ecosystems are also of particular interest because they can act as a secondary source of radioactive contamination for the hydrosphere and other connected systems through hydrological pathways, as still recently exemplified in the territories contaminated by Fukushima atmospheric fallouts (Evrard et al., 2015; Laceby et al., 2016). Finally, the relative contribution of the forest component to the overall internal and external doses to humans, flora and fauna can be significant for populations in close interaction with such environments.

The fate and recycling of deposited radiocaesium in a forest medium is driven by a variety of short to long term biological, physical and chemical processes, some of which are still poorly understood. In the short and mid-term after deposition (months to years), a small part of the activity intercepted by tree canopies can be incorporated mainly into leaves and subsequently translocated to perennial organs, notably wood (e.g. Ronneau et al., 1991; Goor and Thiry, 2004; Nishikiori et al., 2015; Komatsu et al., 2016; Thiry et al., 2016; Gonze and Calmon, 2017). At the same time, a major part of the intercepted deposit is gradually removed and returned to the forest floor through depuration processes such as throughfall, stemflow and litterfall (e.g. Bunzl et al., 1989; Loffredo et al., 2015; Kato et al., 2019). The predominance of return-to-soil fluxes over root uptake is such that forest soil rapidly becomes the main reservoir of radiocaesium activity in the system (Myttenaere et al., 1993; Coppin et al., 2016; Imamura et al., 2017; Gonze et al., 2021; Yoschenko et al., 2022). Radiocaesium activity deposited onto the upper organic layer is more or less rapidly transferred to the upper mineral horizon as a result of organic matter decomposition, lixiviation of mobile physico-chemical forms and biological activity (e.g. Koarashi et al., 2016; Imamura et al., 2017; Takahashi et al., 2018; Muto et al., 2019). Because caesium is efficiently fixed by some specific soil components such as clay particles (Cremers et al., 1988; Wauters et al., 1996; Vandebroek et al., 2012), it only slowly migrates downward and can be retained for a long time in the organic and top mineral layers preferentially colonised by fine roots (Rühm et al., 1999; Jagercikova et al., 2015; Nakanishi et al., 2014; Fesenko et al., 2001a). In contrary to short-term processes that have been well documented and studied after Fukushima accident, the long-term (years to decades) dynamics of radiocaesium remain rather unpredictable due to a lack of understanding and to uncertainties in the parameterization notably of root uptake, bio-chemical factors determining the bioavailability of radiocesium in the rooting soil and internal translocation processes from roots to aerial organs (Hashimoto et al., 2021). Post-Chornobyl studies suggested that the system would reach a quasi-equilibrium state between one and two decades after deposition, which is characterized by an overall balance between root uptake, internal translocation and return-to-soil transfer fluxes (e.g. Tikhomirov and Shcheglov, 1994; Rühm et al., 1999; Goor and Thiry, 2004; Shcheglov et al., 2014). It was also suggested that radiocaesium would be progressively incorporated into the biological cycle of potassium (K), this stable element being considered as a chemical analogue (Yoshida et al., 2004; Varga et al., 2009). This implies that the behaviour and distribution of Cs-137 in the soil-tree system would, to some extent, follow that of potassium in the long-term and/or that of stable caesium (Cs-133). Unlike caesium for which there is no evidence of discrimination between the two isotopes (White and Broadley, 2000), a significant discrimination between Cs-137 and K in root uptake and translocation processes has been evidenced in agricultural crops (Zhu and Smolders, 2000; Casadesus et al., 2008). Thus, analogy with K may be questioned for forest trees. Potassium also acts as a competitor in sorption-desorption in soil as well as in absorption by fine active roots. As such, it can influence the fate of Cs in the soil-tree system. For all these reasons, knowledge of the biogeochemical cycling of K that has long been studied due to its biological importance for plants, as well as that of Cs-133 for which data remain scarce (due to measurement difficulties), is a useful way to make insights into our understanding of long-term dynamics of Cs-137 in terrestrial systems (Rühm et al., 1999; Goor and Thiry, 2004; Yoshida et al., 2004).

Current Cs-137 contamination in French forests originates from both the global fallouts from nuclear weapons test and Chornobyl fallouts, their respective contributions depending on the geographical area considered. Thanks to the RENECOFOR French forest monitoring network, studying the distribution of Cs-137, Cs-133 and K in French beech forests (*Fagus sylvatica* L.) offers the opportunity to bring new lights on the long-term behaviour of Cs-137 for this specific broadleaf deciduous species that is quite common in France. The present study aimed to answer the following questions: How is Cs-137 distributed between forest compartments from 35 to 60 years after initial deposition? To what extent has Cs-137 reached a quasi-equilibrium state? To what extent can we predict the distribution of Cs-137 activity in tree vegetation from K or Cs-133 measurements? Which environmental characteristics might explain the variability observed among sites? To what extent does the bioavailability of Cs-137 in soil determine the contamination in tree organs on the long-term? The present paper is organized as follows. The selected sites, sampling methodology and data treatment are described in sections 2. In sections 3.1 and 3.2, we present and discuss results regarding the distribution of Cs-137, Cs-133 and K concentrations and inventories respectively in soil and tree vegetation, then assess the variability between sites and differences between elements and Cs isotopes. At first, in section 3.3, we quantify the so-called aggregated transfer factor (*Tag*) used in simplistic radioecological assessment studies and discuss our results in the light of the literature. We then characterize the correlation between Cs-137 and stable analogues concentrations for all sites and tree organs. Finally, we attempt to explain the results observed through semi-mechanistic considerations and to estimate Cs/K selectivity coefficients for both root uptake and root-to-shoot translocation processes. The main results are summarized in the conclusion (section 4).

2. Material and method

2.1. Sites characteristics

Soils and beech trees were sampled at three forest sites equipped and monitored by the French National network for long-term monitoring of forest ecosystems (RENECOFOR), which is part of the pan-European network for intensive forest monitoring (ICP Forests level II). The RENECOFOR network has been monitoring 2 ha permanent plots installed throughout France since 1992, regularly collecting data about soil physico-chemical properties, tree growth, atmospheric fluxes, and analyses of major elements in the main biotic and abiotic compartments of forest ecosystems.

The main stand characteristics of the sampled sites are presented in Table 1 and their locations in Fig. 1. These plots differ in the main and secondary trees species and their contributions to the stand basal area. *Fagus sylvatic*a L. (beech) is present in the 3 plots. In the HET site, beech is the dominant tree species, representing 87% of the stand basal area. In the CPS and PS sites, beech is a secondary tree species, accounting for about 1/3 of the stand basal area. The main dominant species on these 2 sites, oaks and pines respectively, accounted for about the 2/3 of the stand basal area. The beech trees in all three sites are quite similar in their average age (from 72 to 89 years), their average diameter at breast height (DBH, from 29 to 37 cm) and their average height (H, from 20 to 27 m). The density of beech trees differs by site: 170 trees ha^{-1} in HET site, 132 trees ha^{-1} in CPS site and 52 trees ha^{-1} in PS site. The sites lay on two contrasted soil types according to the World Reference Base for Soil Resources (IUSS, 2015): (1) eutric cambisol in the HET site with a clayey texture (40% clays) and a mull humus type, and (2) cambic podzol in the CPS and PS sites with a sandy texture (only 4% clays) and a moder humus type. The soils also differ in their organic carbon content, with the highest concentration in the HET and PS sites and a twice as low content in the CPS site.

The sites are under the influence of Temperate Oceanic and Semi-continental climates. Two sources of atmospheric deposition of Cs-137

Table 1
Characteristics of the selected forest sites from the RENECOFOR network.

Site		HET	CPS	PS
Sampling date		2021/01/12	2021/03/09	2021/05/18
Coordinates		43°09′14.1″N 0°39′40.4″W	48°27′15.2″N 2°43′07.4″E	48°51′08.8″N 7°42′20.3″E
Altitude (m) (1)		400	80	175
Slope (%) (1)		44	0	0
Mean annual temperature (°C) (2)		13.3	10.8	10.2
Mean annual precipitations (mm) (2)		1409	698	757
Main dominant species (3)	Tree species	*Fagus sylvatica* L.	*Quercus robur* L. *Quercus petraea* Matt.	*Pinus sylvestris* L.
	Density (trees ha^{-1})	170	98	100
	% of stand basal area	87	59	60
	Mean age (years)	89	133	55
	Mean DBH (cm)	37	56	41
	Mean H (m)	27	28	28
Secondary dominant species (3)	Tree species	*Quercus robur* L. *Quercus petraea* Matt.	*Fagus sylvatica* L.	*Fagus sylvatica* L.
	Density (trees ha^{-1})	6	132	52
	% of stand basal area	7	31	39
	Mean age (years)	–	82	75
	Mean DBH (cm)	65	30	29
	Mean H (m)	–	25	20
Soil organic horizon (1)(4)	Humus type	Mull	Moder	Moder
	Surface density (kg m^{-2})	1.2	1.1	2.5
Soil mineral horizon 0–40 cm (1)(4)	Soil type	Eutric cambisol	Cambic podzol	Cambic podzol
	Clay (%)	40	4	4
	Silt (%)	53	6	13
	Sand (%)	7	90	83
	Organic C (g kg^{-1})	15.4	7.8	18
	Surface density (kg m^{-2})	443	536	495
	pH (H_2O)	4.9	4.8	4.3
	CEC (cmol$^+$ kg^{-1})	6.5	1.0	2.4
Cs-137 atmospheric deposition	Soil inventories (Bq m^{-2})	2812 ± 110	1630 ± 148	3270 ± 208
	Global fallouts (%)	80	84	45
	Chornobyl fallouts (%)	20	16	55

(1) – RENECOFOR report – Soil chemistry (Ponette et al., 1997), (2) – RENECOFOR report – Local weather monitoring (Peiffer et al., 2008), (3) – Estimated trees densities and basal area from RENECOFOR plots, (4) – RENECOFOR report – Soil characteristics (Brêthes and Ulrich, 1997).

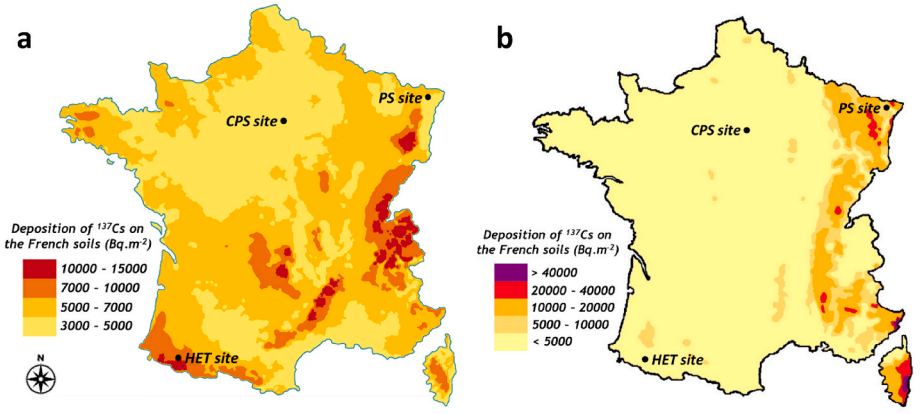

Fig. 1. Atmospheric depositions of Cs-137 on the French metropolitan territory: (a) – nuclear weapons atmospheric tests from 1945 to 1980 (IRSN, 2015) and (b) – Chornobyl accident in 1986 (Renaud et al., 2007).

have impacted the three forest sites: global fallouts from atmospheric nuclear tests (Fig. 1a) and the Chornobyl accident (Fig. 1b). The numerous releases of Cs-137 into the atmosphere from 1945 to 1980 spread over all the French territory (IRSN, 2022). The Cs-137 was mainly deposited in mountainous regions due to the high amount of rainfall. Cs-137 deposits from the Chornobyl accident were more localized in eastern part of France due to unfavourable meteorological conditions, higher activity in air and heavy precipitation prevailing in that part of the country in late April/early May 1986 (Renaud et al., 2007). Hence, respective Cs-137 deposits did not exhibit the same contributions according to site location: PS exhibited the highest total Cs-137 inventories in soil (3270 Bq m^{-2}, Supp. Mat. Table S4.1) and the strongest contribution from the Chornobyl fallouts (55%, Table 1), whereas for HET and CPS sites the global fallouts contributions were estimated to be close to 80% (Table 1), with total soil Cs-137 inventories of 2812 Bq m^{-2} and 1630 Bq m^{-2}, respectively. The contribution of global fallouts to the total amount of Cs-137 activity measured at selected sites was estimated based on the map established by IRSN (2022), the remaining part being attributed to Chornobyl fallouts.

2.2. Sampling and sample treatment

2.2.1. Sampling

Sampling took place in 2021 taking advantage of thinning operations carried out in the immediate vicinity of each of the 3 RENECOFOR monitoring plots. It was performed during the dormant period when all element fluxes have ceased for HET and CPS, but for PS the beech trees had begun to bud. Six trees per site were selected based on DBH distribution of the stands. For the HET site, the DBH population of the dominant trees (beeches, 87% of the basal area) was divided into six DBH classes of equal size and the median DBH of a class was selected (one individual per equal size class). For the CPS and PS sites, two dominant species were considered according to their respective contributions to the stands basal area: the populations of the main dominant species (oaks and Scots pines, respectively) contributing to about 2/3 of the stand basal area were divided into four DBH classes of equal size to select four of these trees in each stand as previously done in the HET site, while the significant contribution of the beech as the secondary dominant species (about 1/3 of the stand basal area) led to select two individuals belonging to the 10th and 90th percentiles of the DBH values of the beech population. Trees with the closest DBH to the median DBH of each considered class were cut for sampling.

Once the trees were cut, the height of the trees was measured. Several stem discs (5 cm thickness) were sampled at four heights of each tree (at 0H, 0.25H, 0.5H, 0.75H) to consider a possible vertical gradient in element concentrations. About 7 kg fw (fresh weight) of branches and 2 kg fw of twigs per tree were randomly taken in the low, middle, and upper parts of the crown to be representative of the developed volume of the entire crown. About 5 kg fw of roots per tree were collected from the stump of each tree: the soil around the roots was removed and once all roots were confirmed as belonging to the selected tree, they were sampled. Later, in July 2021, approximatively 2 kg fw per tree of living leaves were sampled with the same volumetric approach from standing trees, at the same location and with DBH values close to those of the trees sampled during the thinning operation. After their sampling, all the samples were immediately packed and stored for further treatment in the laboratory.

Soil horizons were sampled (N = 6 per stand) close to the sampled trees. The organic layers, i.e. litter (Ol), fragmented (Of) and humified (Oh) ones, were sampled sequentially using the same area frame (0.2 m^2). This approach was adopted due to the difficulty of coring through branches in the litter, its variable thickness, and low bulk density. The organic horizon was separated into litter (Ol) and a single fragmented + humified layer (Of + Oh) due to the difficulties in distinguishing them. After *in-situ* removal of the organic layers, cores of the mineral layer were taken with a cylindric auger (9.7 cm of internal diameter, 10 cm length) down to a depth of 40 cm to account for the total inventory of Cs-137 in soil. Each soil core was divided into 0–10 cm, 10–20 cm and 20–40 cm layers to fit with the RENECOFOR soil sampling method (see Ponette et al., 1997). As low Cs-137 concentrations were expected below 20 cm mineral soil depth (Baeza et al., 2005; Konopleva et al., 2009; Yoschenko et al., 2017), it was also considered more relevant to collect the 20–30 cm and 30–40 cm mineral layers together.

2.2.2. Samples treatment

Once in the laboratory, stem discs, bark, branches, and twigs were first brushed to remove lichens and mosses and then rinsed with tap water. The same process was applied to the roots to remove soil particles until the soil was no longer detectable when blotted with white paper. The roots were then divided into three diameter (Ø) classes: <1 cm, 1–3 cm and >3 cm. All samples were rinsed with reverse osmosis water to remove any residual elementals from their surface. Leaves were only rinsed with mineral-free water. For the stem compartments, a disc sector (see Supp. Mat. Figure S1) was sampled in the same proportion from each stem disc per tree (0H, 0.25H, 0.5H, 0.75H). Each disc sector was further separated into four compartments: outer bark, inner bark, sapwood, and heartwood. Then the samples taken from the 4 discs were pooled into one composite per stem compartment and per tree. All the vegetal samples were oven-dried at 70 °C until constant weight. To further concentrate these dry samples, they were decarbonised in a furnace to obtain white ashes (Supp. Mat. Table S1). The dry samples of outer bark and leaves were ground directly due to the low amounts of ash expected as compared to the amount of dry sample to be processed.

A single composite sample per soil layer (Ol, Of + Oh, mineral 0–10 cm, 10–20 cm, 20–40 cm) and per site was made. In the laboratory, coarse gravels, stones, and roots were removed from the mineral soil samples (sieving mesh 2 mm). Each soil sample was dried at 105 °C and then homogenized. The Cs-137, Cs-133 and K exchangeable fractions were extracted using 1M ammonium acetate (NH_4Ac) with a solid to liquid ratio of 1:10 (Teramage et al., 2018): the NH_4Ac solution (4 L) was added to 400g of samples of the 0–10 and 10–20 cm mineral soil layers, then mixed and shaken with a rotary agitator at 11 rpm (Heidolph, Reax 20–8) for 21 h. Because of an extraction yield expected <10% (Fesenko et al., 2001b; Konopleva et al., 2009), the 0–10 cm and 10–20 cm mineral soil layers were used because of the expected highest Cs-137 concentrations in these layers. After 3 h of decantation of the solid particles, 3 L of supernatant was filtered with 0.45 μm cellulosic ester filters and placed in 3L Marinelli container for further gamma-spectrometry analyses. An aliquot of ~50 mL was sampled and stored for further ICP-MS and ICP-AES analyses. Data of total Cs-133 and K contents in the 0–20 cm and 0–40 cm mineral soil layers were obtained from the RENECOFOR database. Their procedure to reach the structural mineral pool of soil elements consisted in a complete dissolution of the soil solid matrix performed by calcination at 450 °C followed by digestion with both hydrofluoric acid (HF) and perchloric acid ($HClO_4$) according to the EU referenced French norm NF X31-151 (see Ponette et al., 1997).

For the analysis of stable analogues contents (Cs-133 and K) in the vegetal compartments, approximately 0.1 g of homogenized aliquots of ash samples were taken and dissolved in 50 mL of HNO_3 4%, then left to stand for several hours to separate the solution from the solid particles (decantation). The supernatant aliquot was taken and filtered with double 0.8/0.2 μm PF (Hydrophilic polyethersulfone) filters. Filtered solution was further diluted with UHQ water to reach a final concentration of HNO_3 2% (m/m) and stored at 4 °C until analysis. Dry samples (outer bark, leaves) were mineralized with a microwave digester (CEM MarsXpress5): 0.5 g aliquots were mixed with 6 mL HNO_3 69%, 3 mL HCl 37% and 1 mL UHQ water. These solutions were digested at 180 °C for 30 min. Once digested, all samples were filtered with 0.2 μm PF filters, then filtrate was evaporated. The dry extract was homogenized with HNO_3 2% (m/m) then stored at 4 °C until analysis.

2.3. Analytical measurements

2.3.1. Cs-137

Cs-137 activities were measured by gamma-spectrometry with HPGe Coaxial Radiation Detector (Eurisys-Mesures, reference: EGPC 42–190R; 40% of relative efficiency). For vegetation ash samples the detection limit (DL) was 0.20 Bq per sample with 8 h of counting in 120 mL geometry. If measurement was below this DL, the samples were re-measured for 24 h with a lower DL (0.08 Bq per sample). If the results were again below this second DL, a composite sample was performed. The dry vegetation samples were measured in 500 mL containers and the detection limits were 0.10 Bq and 0.08 Bq per sample with 12 and 24 h of counting, respectively. The reference date for the results of gamma-spectrometry analysis of vegetation samples was set to the date of sampling in the corresponding stand (Table 1).

The dry soil samples were measured in 500 mL containers with the same detector as mentioned above. The detection limits were 0.10 Bq and 0.08 Bq per sample with 12 and 24 h of counting, respectively. The NH_4Ac extracted soil solutions were analysed in 3 L Marinelli beakers for 24 h with a DL of 0.10 Bq per sample. The reference date for gamma-

spectrometry of soil samples was setup to 2020/09/01.

2.3.2. Cs-133 and K

For all vegetal samples, stable caesium and potassium concentrations were determined by ICP-MS (Agilent 7800, Agilent Technologies, Tokyo, Japan) and ICP-AES (OPTIMA 4300 DV, PerkinElmer), respectively. To prepare calibration solutions, 1000 mg L^{-1} standard solutions of Cs-133 and K purchased from PlasmaCAL (SCP Science) were used. Instrumental quantification limits (Cs-133: ~1 ng L^{-1}; K: ~10 µg L^{-1}) were obtained from external calibrations in HNO3 4% with analytical precision <10%.

2.4. Data processing

2.4.1. Soil density and elements inventories in soil

For the soil organic layers, the total dry mass (kg dw) was divided by the area of the sampling frame (m^2) to obtain the mass density of each layer per site (kg dw m^{-2}). For the mineral soil layers, the dry mass of the fine earth <2 mm (kg dw) was divided by the volume of the auger (m^3) to obtain the volumetric mass density of each mineral soil core (kg m^{-3}). Then the volumetric mass density was multiplied by the thickness of the related layer to obtain the mass density per site (kg dw m^{-2}). For each soil layer, the mass density was further multiplied by the concentrations of elements (Bq or g kg^{-1}) to estimate the element inventories or stocks per soil layer (Bq or g m^{-2}).

2.4.2. Cs-137 exchangeable fraction in soil mineral horizon

The NH_4Ac extracted and total Cs-137 concentrations were used to calculate the exchangeable fraction of this element in the 0–20 cm mineral soil layer (expressed in %) with Equation (1). This percentage was then applied to the inventories of each mineral soil layer to obtain the exchangeable fraction inventory of the 0–40 cm mineral soil layer (in Bq m^{-2}).

$$Exchangeable\ fraction = \frac{\left[^{137}Cs\right]_{extracted} \times V_{extraction}}{\left[^{137}Cs\right]_{0-20cm} \times M_{soil}} \times 100 \quad (1)$$

where $\left[^{137}Cs\right]_{extracted}$ is the concentration of extracted Cs-137 (Bq L^{-1}), $\left[^{137}Cs\right]_{0-20cm}$ is the Cs-137 concentration in the 0–20 cm soil layer (Bq kg^{-1} dw) and $V_{extraction}$ is the extraction volume (4 L) and M_{soil} the mass of soil (0.4 kg dw).

2.4.3. Biomass of trees compartments

Specific stem discs were used for biometric measurements (Supp. Mat. Figure S1). The width of the outer bark, inner bark, sapwood, and heartwood rings was measured on 4 axes, i.e. 8 radius, of each stem disc to model the volume of the tree stem according to a truncated cone model, and to acquire biomass allocation factors in the stem.

The mass density of each compartment (kg dw m^{-3}) was determined to allow the calculation of the stem compartment biomass. This estimated biomass was then compared with those obtained from models based on the allometric equations from the literature for beech trees (e.g. Bartelink, 1997; Genet et al., 2011; Chakraborty et al., 2016; Calvaruso et al., 2017). The model by Genet et al. (2011) showed the best agreement between modelled and estimated stem biomasses (Supp. Mat. Figure S2). This model was used to predict the biomass of foliage, branches, bark, stem and roots as given by the following allometric relationships:

$$Biomass_i^p = \alpha + \beta \times \left(DBH^2 \times H\right)^{\gamma} \quad (2)$$

where $Biomass_i^p$ (kg dw per tree) is the biomass of the given organ i for any tree p, DBH (m) is the tree diameter at breast height, H (m) is the tree height and α, β, γ are unitless model parameters (given in Supp. Mat. with Figure S2). DBH and H values are released in Supp. Mat. Table S2. Then, outer bark, inner bark, sapwood, and heartwood biomasses were obtained by applying allocation factors acquired from biometrics on stem disk. Finally, twig biomass was estimated from the ratio of twig to branch biomass (0.0018) derived from Devillez et al. (1973). To obtain a representative biomass density of tree vegetation at the scale of the plot, denoted $Biomass_i$ (kg dw m^{-2}), the individual biomasses were summed over the tree population and normalized by the plot area S (5000 m^2).

2.4.4. Concentration and inventory of elements in trees

To account for the variability of tree biomass between individuals, the mean element concentration of Cs-137, Cs-133 and K in tree organ i, denoted $[Element]_i$ (Bq or g kg^{-1} dw), was calculated as the weighted-average concentration over sampled individuals p:

$$[Element]_i = \frac{\sum_p [Element]_i^p \times Biomass_i^p}{\sum_p Biomass_i^p} \quad (3)$$

Where $[Element]_i^p$ (Bq or g kg^{-1} dw) is the concentration in tree p.

Element inventory in any tree organ i at the scale of the plot, denoted $StockElement_i$ (Bq or g m^{-2}), was calculated by multiplying the mean concentration $[Element]_i$ by the biomass density $Biomass_i$.

2.4.5. Concentrations normalized by the soil exchangeable fraction inventory (NCE)

Mean element concentrations in tree compartments were normalized by the exchangeable fraction inventory of the element considered in the 0–40 cm mineral soil layers (Equation (4)), hereafter referred to as *NCE*, to compare the results between sites.

$$NCE\ Element_i = \frac{[Element]_i}{StockElement_{soil\ exchangeable}} \quad (4)$$

where $StockElement_{soil\ exchangeable}$ is the inventory of the exchangeable fraction in the 0–40 cm mineral soil layer (Bq or g m^{-2}).

2.4.6. Statistical analyses and uncertainties calculation

Statistical analyses were performed with the R software (R Core Team, 2013; version 4.1.3). Pearson's test was used to assess linear correlations between normalized concentrations of Cs-137, Cs-133 and K.

The uncertainties attached to the concentrations correspond to the analytical uncertainties. Uncertainties in concentrations, inventories, exchangeable fractions in mineral soils and normalized concentrations, were classically propagated.

2.5. Semi-mechanistic modelling of Cs-137 root uptake by tree vegetation

To shed a little more light on the expected relationships between Cs-137 and stable analogues concentrations in tree vegetation induced by root uptake, some "theoretical" considerations were developed. As discussed in several publications (e.g. Myttenaere et al., 1993; Sombré et al., 1994; Berg and Shuman, 1995; Zhu and Smolders, 2000; Goor and Thiry, 2004; Casadesus et al., 2008; Rantavaara et al., 2012; Kobayashi et al., 2019), the uptake of Cs-137 by roots can be reasonably related to the annual demand for K of growing vegetation, $UpK(t)$ (gK m^{-2} d^{-1}), divided by the characteristic concentration of exchangeable K, $[K]$ (gK kg^{-1} dw). Such a ratio quantifies the "driving force" of the root uptake mechanism. Based on this assumption, the root uptake flux of Cs-137 from each rooting soil layer j ($Up^{137}Cs_j$ in Bq m^{-2} d^{-1}) can be expressed as follows:

$$Up^{137}Cs_j = sel^{up} \times \frac{UpK \times \alpha_j^{up}}{[K]_j} \times \left[^{137}Cs\right]_j \quad (5)$$

Where $[^{137}Cs]_j$ is the concentration of exchangeable Cs-137 in layer j (Bq kg^{-1} dw), $[K]_j$ is the concentration of exchangeable K in j (gK kg^{-1} dw), sel^{up} (n.d.) is the Cs/K selectivity coefficient specific to root absorption

(comprised between 0 and 1) (n.d.) and α_j^{up} (n.d.) quantifies the proportion of K which comes from j (n.d.). By definition, $\Sigma\alpha_j^{up} = 1$ (summation over layers j). If K concentration is constant with depth, α_j^{up} approximately corresponds to the density of fine absorbing roots (Ø < 2 mm). We can further assume that Cs-137 up-taken by roots is less efficiently translocated to aboveground organs than K, because of chemical discrimination in the internal transfer processes. If discrimination is efficient, Cs-to-K concentration ratio in aerial organs should be significantly smaller than in roots. Based on the previous assumptions (to be confirmed at field), we obtain the following approximation for Cs-137 concentration in any aerial organ i:

$$\left[^{137}Cs\right]_i \sim sel_i^{tra} \times sel^{up} \times \frac{[K]_i}{[K]} \times \Sigma\, \alpha_j^{up} \times \left[^{137}Cs\right]_j \quad (6)$$

Where sel_i^{tra} (n.d.) is the Cs/K selectivity coefficient (between 0 and 1), $[K]_i$ (gK kg^{-1} dw) denotes K concentration in organ i and $[K]$ (gK kg^{-1} dw) denotes the constant concentration in soil. In a first approximation, we will consider that selectivity is identical for all aerial organs. As a result of stock definition, Equation (7) can be reformulated as follows:

$$\frac{\left[^{137}Cs\right]_i}{Stock^{137}Cs} \sim sel^{tra} \times sel^{up} \times \frac{[K]_i}{StockK} \times \Sigma\, \frac{\alpha_j^{up} \times \beta_j}{w_j} \quad (7)$$

Where $Stock^{137}Cs$ is the total stock of exchangeable Cs-137 in the rooting zone (Bq m^{-2}), $StockK$ is the corresponding stock of exchangeable K (gK m^{-2}), β_j (n.d.) is the contribution of layer j to the total inventory of Cs-137 in the rooting zone and w_j (n.d.) is the contribution of layer j to the total mass density of the rooting zone expressed in kg dw m^{-2}. By definition, we have $\Sigma\beta_j = \Sigma w_j = 1$. The last right-hand side (RHS) term of Equation (8) quantifies the effect of vertical inhomogeneities while the net selectivity coefficient, $sel^{tra} \times sel^{up}$, quantifies the cumulated effect of selectivity in root uptake and translocation.

The previous theoretical reasoning can be applied to Cs-133 except that we consider here that there is no isotopic discrimination between Cs-137 and Cs-133, that is: $sel^{up} = sel^{tra} = 1$. Thus, normalized concentration of exchangeable Cs-137 in aerial organs can be simply estimated from Cs-133 concentration as follows:

$$\frac{\left[^{137}Cs\right]_i}{Stock^{137}Cs} \sim \frac{\left[^{133}Cs\right]_i}{Stock^{133}Cs} \times \Sigma\, \frac{\alpha_j^{up} \times \beta_j}{w_j} \quad (8)$$

where the last RHS term is identical to that for K.

As long as the contribution of foliar uptake is negligible with respect to root uptake's, this modelling approach tells us that NCE Cs-137 and NCE Cs-133 or K would be related in a linear way, the proportionality coefficient depending on vertical inhomogeneities in the rooting zone and selectivity coefficients (for K). If the mean vertical distribution of fine roots density is measured at site, reliable estimations of Cs-137/K regression slopes for both aerial and root organs enable to infer the two selectivity coefficients. If *in situ* measurement of element concentrations in roots or root density profile are not reliable enough, one can nevertheless evaluate the net selectivity coefficient, $sel^{tra} \times sel^{up}$, by comparing regression slopes obtained for Cs-137/K and Cs-137/Cs-133 relationships.

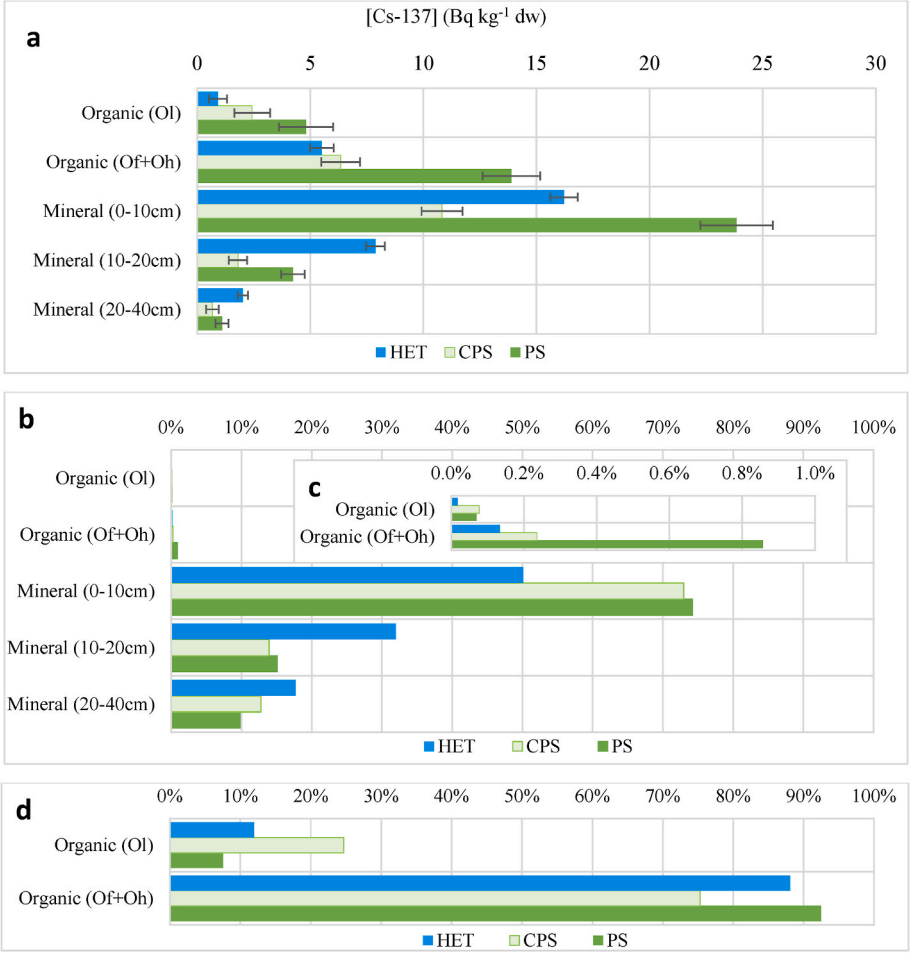

Fig. 2. (a) – Concentration of Cs-137 in organic and mineral soil horizons, error bars correspond to 1 standard deviation. (b,c) – Contribution of each soil layer to the total inventory of Cs-137 in soil. (d) Contribution of each organic layer to the total inventory of Cs-137 in the organic soil.

3. Results & discussion

3.1. Vertical distribution of Cs-137 and stable analogues contents in forest soil

3.1.1. Cs-137 concentrations and inventories

The Cs-137 concentrations in soils were heterogeneously distributed among soil layers (Fig. 2a, Supp. Mat. Table S3.1) with the highest concentrations in the mineral soil layer 0–10 cm at each site (11–24 Bq kg^{-1} dw) and then decreasing with depth in the mineral horizon. In the organic horizon, the Of + Oh layers had higher Cs-137 concentrations (5.5–14.0 Bq kg^{-1} dw) than the Ol layer (0.9–5.0 Bq kg^{-1} dw) at all sites. The mean ratio of Cs-137 concentrations between the Of + Oh and the 0–10 cm mineral layers were around 0.3, 0.6 and 0.6 for HET, CPS and PS, respectively, i.e. twice greater in CPS/PS than HET sites. In the study carried out by Winkelbauer et al. (2012) 25 years after the Chornobyl fallouts in Bavarian forests (southern Germany), this ratio was 3 times greater in stands characterized by moder humus type (like CPS, PS) than mull humus type (like HET), i.e. a ratio of 3.3 in moder humus (N = 15, excluding pure coniferous stands) vs. 1.1 in mull humus soil (N = 14). The slower humification process and turnover of moder humus type (Ponge, 2003; Karroum et al., 2005) could explain the higher retention of Cs-137 in the organic layers.

For the three forest sites, the organic horizon accounted for less than 1% of the total soil Cs-137 inventory (Fig. 2b,c), i.e. 35 years after the Chornobyl accident, with a major contribution coming from the Of + Oh layer (75–92%) (Fig. 2d). The latter result is in line with the reported contributions observed by Belli et al. (2000) in European forest stands about 10 years after the Chornobyl accident. Such a low contribution of the organic horizon to the soil Cs-137 inventory differs from that observed around 10 years after Chornobyl accident in Ukraine and Russia or even 5 years after the Fukushima accident, where the organic horizons contributed 11–91% of the total soil Cs-137 inventory (Krasnov, 1999; Shcheglov et al., 2001; Imamura et al., 2017). The decrease of the organic layers contribution to the Cs-137 inventory in soil according to the time elapsed from deposit in forest stands is consistent with the continuous decrease of Cs-137 concentrations in crown compartments (Mamikhin and Klyashtorin, 2000; Clouvas et al., 2007; Imamura et al., 2017; Tsvetnova et al., 2018; Kato et al., 2019; Hashimoto et al., 2021) and canopy to forest floor fluxes (Kato et al., 2019) over time, as root uptake supply could not compensate for field losses (litterfall, crown leaching, weathering) and biomass growth (Gonze et al., 2021).

As also shown in Fig. 2b, significant differences in the contributions of organic horizons to the total Cs-137 inventory exist between forest stands, with the lowest contributions for the HET and CPS sites (~0.2 and 0.3 %, respectively) and the highest one for the PS site (~1%). The higher retention of Cs-137 at PS site likely results from a higher mass density of the Of + Oh layer in this stand dominated by conifers (2.0 kg dw m^{-2} *vs.* 0.7 and 0.6 kg dw m^{-2} at HET and CPS sites, respectively, Supp. Mat. Table S3.1). Climatic characteristics and litter composition are the main factors influencing litter decomposition and organic matter turnover (Zhang et al., 2008), the latter factor itself depending on the nature of litterfall debris and the tree species abundance. At CPS and PS sites, oaks and pines are respectively the major contributors to the organic horizon material. The highest contribution of organic layers (Fig. 2d) might be explained by a slower turnover of organic matter than expected in purely deciduous stands. To some extent, this might also result from a relative contribution of Chornobyl fallouts higher than at HET and CPS sites (Table 1), this resulting *a priori* in higher Cs-137 concentrations in canopy organs and return-to-soil Cs-137 fluxes than at sites contaminated by older global fallouts. The slight difference between pure deciduous HET and CPS sites, where the contributions of global fallouts were similar, could be explained by higher Cs-137 concentrations in canopy organs at CPS (Supp. Mat. Table S3.2), site-specific climatic parameters as well as the nature of the organic matter (mull vs. moder) as previously discussed.

Despite some disparity between sites, the main Cs-137 inventories were confined to the first 10 cm of the mineral soil irrespective of the site (Fig. 2b) as was also observed by Konopleva et al. (2009) in southern German forests investigated 19 years after the Chornobyl accident. About 50% of the total Cs-137 inventory had migrated below 10 cm at HET site (cambisol), whereas only 25–27% was found below 10 cm at CPS and PS sites (podzol). The vertical profiles of Cs-137 inventory displayed in Fig. 2b are typical of those in undisturbed soil layers (Belli, 2000; Jagercikova et al., 2015; Koarashi et al., 2023) due to the low mobility or downward migration of Cs-137 with characteristic velocities of typically 0.2–0.3 cm y^{-1} (IAEA, 2010). In soils, Cs-137 is quasi-irreversibly adsorbed on the Frayed Edge Sites (FES) of clays (Kruyts and Delvaux, 2002) due to their high absorption selectivity for Cs cations (Cremers et al., 1988; Wauters et al., 1996; Vandebroek et al., 2012) and diffuses from the FES through the interlayer space of clays reducing its mobility over time (Kruyts and Delvaux, 2002). In their meta-analysis of vertical migration of Cs-137 in a variety of forest soils, Jagercikova et al. (2015) obtained twice higher velocities in cambisol than in podzol soils. This corroborates our observations. The modeling study of Jagercikova and co-authors (2015, 2017) concluded that downward migration was mainly correlated to the solid transportation of clay particles, which is itself sensitive to percolating water intensity (Quénard et al., 2011), through preferential flow paths notably. In this regard, the significantly higher annual rainfall amount at HET site (1409 mm) compared to CPS and PS (698 and 757 mm, respectively, Table 1) should have enhanced lixiviation of Cs-137 in the mineral profile.

Homogenization of the mineral soil layers through bioturbation by soil macrofauna (e.g. endogeic and anecic earthworms) could also explain the long-term deeper migration of Cs-137 in cambisol (HET) than in podzol (CPS/PS). Based on experiments aiming at monitoring N-15 vertical profiles in forest soils supplied by N-15 enriched litterfall, Nicolas et al. (2006) and Salleles (2014) concluded that the higher biological activity of burrowing earthworms in forest soils under mull humus explain the faster vertical mixing of N-15 when compared with moder humus. More, the earthworm galleries in soil create preferential flow paths that enhance downward transportation of solutes and solid particles as discussed previously. On another hand, according to Sakashita et al. (2020), the fine roots (Ø < 2 mm) turnover may have contributed significantly to the downward migration of Cs-137 in forest mineral soil layers. Indeed, the mortality of fine roots, which is of the same order of magnitude as or even greater than the current living fine roots biomass (Lwila et al., 2023), is a major process of organic matter input into mineral soil layers (Jonard et al., 2017; Heinze et al., 2018). In Japanese beech (*Fagus crenata* Blume) stands contaminated by ca. 95% of global fallouts, Koarashi et al. (2023) showed that, in the long-term, the retention ratio in the mineral soil was negatively correlated with the soil organic carbon concentration. However, the significance of the fine root turnover process could not be demonstrated in the current study and remains to be assessed with field investigations by accounting for the rooting system morphology and the fine roots dynamics. Anyway, both abiotic (clays leaching) and biotic (bioturbation, roots mortality) processes need to be further documented to better quantify their respective contributions to Cs-137 migration in forest soils, especially in the long-term.

3.1.2. Stable analogues concentrations and inventories

In contrast to Cs-137, Cs-133 and K concentrations in the mineral soil layers were uniformly distributed in the mineral profiles at all sites (Fig. 3a and b, Supp. Mat. Table S3.1). Mean Cs-133 concentrations in mineral horizons varied from 0.8 to 8.0 mg kg^{-1} dw depending on the forest site and were in the range of values reported by Burger and Lichtscheidl (2018) for soils, i.e. 0.3–25 mg kg^{-1} dw. Cs-133 concentrations were 3–4 orders of magnitude lower than those of K, ranging within 8–15 g kg^{-1} dw in agreement with those derived from the review

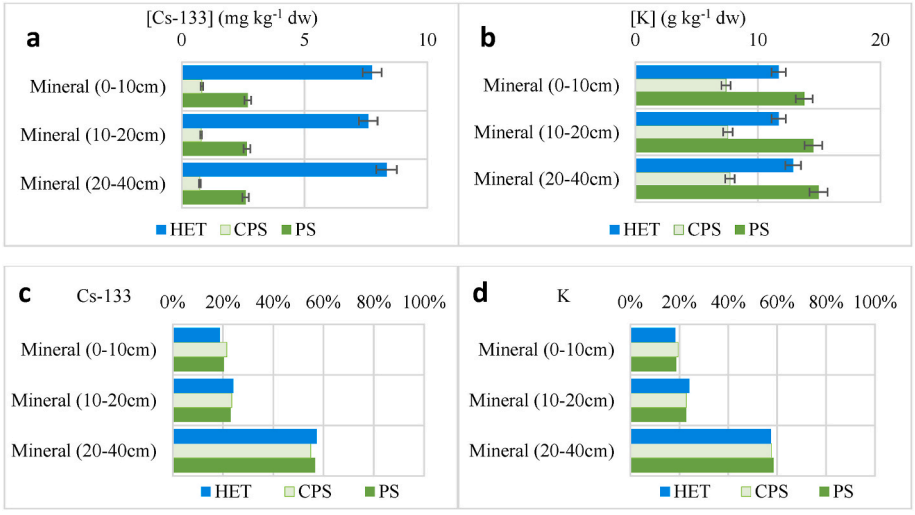

Fig. 3. (a,b) – Concentrations of Cs-133 and K in mineral horizons, respectively, error bars correspond to 1 standard deviation. (c,d) – Contribution of each mineral horizon to the total inventory in mineral soil for Cs-133 and K, respectively.

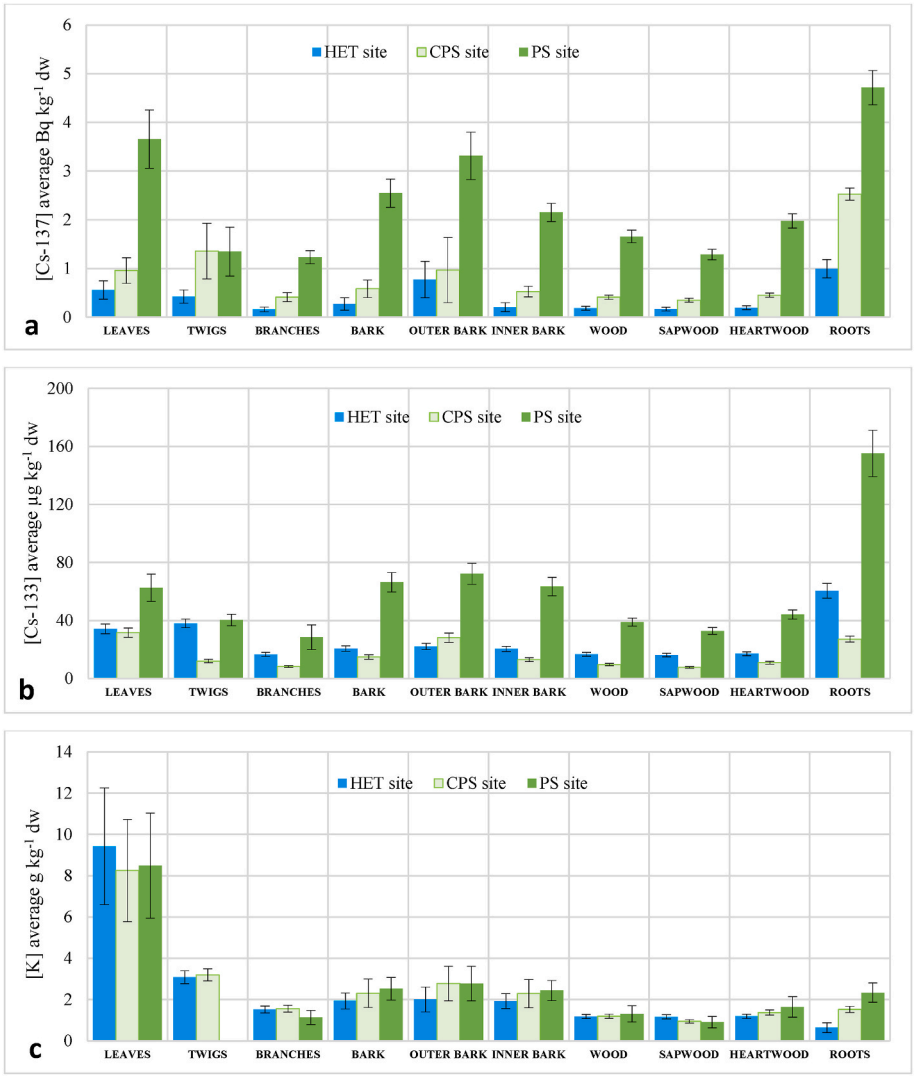

Fig. 4. (a,b,c) – Concentrations of Cs-137, Cs-133 and K in beech tree organs, respectively ([K] in twigs not determined at PS). Error bars correspond to 1 standard deviation.

of Sardans and Peñuelas (2015).

HET site had the highest Cs-133 inventories in the mineral soil (3590 mg m^{-2} dw, Supp. Mat. Table S4.1), followed by PS (1350 mg m^{-2} dw) and CPS (420 mg m^{-2} dw). In contrast to Cs-133, the highest K inventories were found at PS site (7440 g m^{-2} dw), followed by HET (5513 g m^{-2} dw) and CPS (4150 g m^{-2} dw). Nevertheless, the distribution of K (Fig. 3d) between the mineral layers was very similar to that of Cs-133 (Fig. 3c). The vertical profiles of Cs and K inventories were characteristic of their respective origins, i.e. atmospheric for Cs-137 (Fig. 2b) and geogenic for Cs-133 and K (Fig. 3c and d). Both Cs-133 and K are mainly provided by soil mineral weathering (White and Broadley, 2000) and their distributions vary little over depth (Fig. 3c and d) (Ranger et al., 1995a; Marques et al., 1997; Yoschenko et al., 2022).

3.1.3. Exchangeable fractions of Cs isotopes and K

The concentrations of exchangeable Cs-137 in the mineral soil (0–40 cm) were in the range 0.12–0.50 Bq kg^{-1} dw (Supp. Mat. Tab. S3.1). On average, the exchangeable fraction of Cs-137 was about 8% at HET and PS sites against 4% at CPS site. These values were in agreement with those acquired with the same protocol (NH_4Ac) by Fesenko et al. (2001b) about 10 years after the Chornobyl accident in mineral A layers of soddy-podzolic loamy sands under Scots pines stands, typically ranging from 1 to 10 %.

The mean exchangeable Cs-133 and K concentrations in the mineral soil were respectively in the range 0.02–0.27 mg kg^{-1} dw and 12–45 mg kg^{-1} dw. The Cs-133 exchangeable fractions amounted to 3.4%, 2.7% and 1.7% at HET, CPS and PS sites, respectively. The exchangeable fraction of K was estimated to 0.5%, 0.3% and 0.1% at HET, CPS and PS sites, respectively. An order of magnitude difference between the relative abundance of Cs-133 and K exchangeable fractions (%) was assumed to be due to the structural abundance of K in primary minerals (Sparks and Huang, 1985; Sardans and Peñuelas, 2015) which mechanically decreased the ratio of K exchangeable inventory to its total inventory.

3.2. Cs-137 and stable analogues contents in beech trees

3.2.1. Cs-137 concentrations

Concentrations of Cs-137 in beech organs (Fig. 4a) varied by more than an order of magnitude between sites and organs, ranging from 0.2 to 4.7 Bq kg^{-1} dw (Supp. Mat. Table S3.2). For all sites, the ranking of organs was very similar: roots > outer bark ~ leaves ~ twigs ≥ heartwood ~ sapwood ~ branches ~ inner bark. Roots (1.0–4.7 Bq kg^{-1} dw), outer bark (0.8–3.3 Bq kg^{-1} dw), leaves (0.6–3.7 Bq kg^{-1} dw) and twigs (0.4–1.4 Bq kg^{-1} dw) generally showed the highest concentrations, except for twigs at PS site which were in the same range as branches. On the contrary, branches (0.2–1.2 Bq kg^{-1} dw), wood (0.2–1.7 Bq kg^{-1} dw) and inner bark (0.2–2.2 Bq kg^{-1} dw) generally showed the lowest concentrations. Contrasting with what was observed in the short-term period after an accident, the variability of Cs-137 concentrations between tree organs was found to be small, typically contained within a factor of 3.

A decade after the Chornobyl deposit, Fesenko et al. (2003) also found a similar ranking of Cs-137 concentrations in birch organs (roots > leaves > bark > wood), notably with roots exhibiting the highest Cs-137 concentrations among the measured organs. In the study by Tsvetnova et al. (2018) of Cs-137 contamination in birch (*Betula* spp.) and oak (*Quercus* spp.) stands, the variability among organs observed 24 years after Chornobyl was contained within 3–4 orders of magnitude, with concentrations being the highest in outer bark and the lowest in wood. When the analysis was restricted to the other organs (leaves, twigs, branches, roots and inner bark), the variability was reduced to less than a factor of 5, closer to what we observed. The very high contamination of the outer bark from the study by Tsvetnova et al. (2018) was probably due to the strong remanence of the intercepted atmospheric fallouts resulting from a slow turnover of the stem bark and/or low stemflow outputs. To our knowledge, stem bark turnover data are unfortunately scarce to assess this hypothesis and vary according to tree type as illustrated by Paul et al. (2022): In this modelling study, half-lives were estimated to vary from 89 to 194 years for softwood (coniferous) species (N = 138), mainly represented by *Pinus* spp. and from 5.4 to 15.7 years for hardwood (deciduous) species (N = 80), mostly represented by *Eucalyptus* spp. These data may not be applicable to beech trees, as they appear to be very specific to the tree species considered and don't allow a reliable calculation of the remaining contamination inventory in the outer bark over time. The ranking of Cs-137 concentrations released by Tsvetnova et al. (2018) also differed from that of our study and are as follows for birch and oak trees, respectively: (birch) outer bark > twigs ~ leaves > inner bark ~ roots > branches > wood and (oak) outer bark > roots > leaves > branches ~ inner bark > twigs > wood. These results suggest a tree species effect, as well as those from the study of Fogh and Andersson (2001) in forests of the Bryansk region investigated about 10 years after Chornobyl accident when comparing the ranking of Cs-137 concentrations in aboveground organs between birch trees (leaves > twigs ~ wood > branches) and oak trees (leaves > bark > branches ~ twigs > wood). The scarcity of Cs-137 time series data in forest stands doesn't allow distinguishing accurately the variability generated by species effect from that due to the time elapsed from deposit in the stand of the current study even if global patterns were identified.

Another noticeable result from Fig. 4a (Supp. Mat. Table S3.2) was the absence of significant difference between Cs-137 concentrations in sapwood and heartwood. Heartwood is a dead lignified cells tissue where nutrients are immobilized and resorption occurs during its formation from senescing sapwood (Meerts, 2002). This process creates a net flux of elements from heartwood to sapwood, resulting in higher Cs-137 concentrations in sapwood as demonstrated in post-Chornobyl studies (Sombré et al., 1994; Goor and Thiry, 2004; Yoshida et al., 2011). Ten years after the Chornobyl accident, Fesenko et al. (2001a) measured Cs-137 concentrations in birch wood that decreased from the outer (sapwood) to the inner (heartwood) stem rings by one order of magnitude, while Holiaka et al. (2023) observed the opposite trend (sapwood < heartwood) more than 30 years after the Chornobyl in birches grown in Chornobyl Exclusion Zone. In this latter study, Scots pines exhibited an opposite gradient with respect to birch trees (sapwood > heartwood). Such a dependence on tree species was still again observed after the Fukushima accident by Ohashi et al. (2017, 2020) who revealed quite contrasting patterns between the different species studied (Japanese cedar and cypress, Konara oak, larch, red pine).

3.2.2. Stable analogues concentrations

The Cs-133 concentrations in beech organs ranged from 8 to 155 μg kg^{-1} dw (Supp. Mat. Table S3.2). In all stands, the highest concentrations were found in roots (27–155 μg kg^{-1} dw) or leaves (32–63 μg kg^{-1} dw), whereas the lowest concentrations were found in branches (8–28 μg kg^{-1} dw) or wood (10–39 μg kg^{-1} dw). The ranking of tree organs was very similar to that observed for Cs-137 (Fig. 4a and b, Supp. Mat. Table S3.2): roots ≥ leaves ~ outer bark ~ inner bark > twigs ≥ branches ~ sapwood ~ heartwood. The two peculiarities of the Cs-133 distribution are: non-significant differences between outer bark and inner bark (for HET and PS) and leaves > twigs (for CPS and PS). Despite these slight discrepancies, the Cs-133/Cs-137 ratio was fairly constant between organs at each site (Coefficient of variation of 0.3, 0.4 and 0.2 for HET, CPS and PS sites, respectively, data not shown). Yoshida et al. (2011) reported a similar distribution of both Cs isotopes in stem of Scots pines 12 years after Chornobyl accident. This was also corroborated by Yoschenko et al. (2018) measurements in the stems of Japanese cedars 3 years after the Fukushima accident, i.e. showing a constant Cs-133/Cs-137 ratio (see also Yoshida et al., 2004). Cs-133 concentrations were the highest at PS site but, in contrast to Cs-137, they were

generally higher at HET than CPS (Fig. 4b). The reasons behind this remain unclear as Cs-133 is assumed to be exclusively supplied to tree from the soil and none of the soil or eco-physiological parameters measured in this study can explain such a difference in root transfer.

K concentrations were about 5 orders of magnitude higher than Cs-133 concentrations in beech organs (Fig. 4c–Supp. Mat. Table S3.2), whereas the difference did not exceed 3 to 4 orders of magnitude in the forest soils (see previous section). Such a contrast probably resulted from a discrimination between Cs and K in root absorption. Contrary to Cs isotopes (Fig. 4a and b), no significant difference between sites could be detected for individual organs, except for roots, which did not show such a relatively high element concentration for K. Leaves were the main sink for K, exhibiting the highest concentrations (8.2–9.4 g kg^{-1} dw) regardless the site, followed by twigs (ca. 3 g kg^{-1} dw), then bark organs (2.0–2.8 g kg^{-1} dw and 1.9–2.4 g kg^{-1} dw, for outer bark and inner bark, respectively). The lowest K concentrations were found in the lignified compartments, i.e. branches (1.1–1.6 g kg^{-1} dw), sapwood (0.9–1.2 g kg^{-1} dw), heartwood (1.2–1.6 g kg^{-1} dw) and roots (0.6–2.3 g kg^{-1} dw). Generally, we did not observe significant differences between outer bark and inner bark as well as between sapwood and heartwood. The variability of K concentrations among organs (excluding leaves) was contained within a factor of 3 (PS, CPS) to 5 (HET). The highest K concentrations were often found in leaves of deciduous trees or in coniferous needles (Ranger et al., 1995b; Sardans and Peñuelas, 2021). Tsvetnova et al. (2018) found a slightly different distribution of K concentrations in birch and oak trees growing on close soil substrates: (birch) leaves > twigs > inner bark ~ roots > branches > outer bark ~ wood and (oak) leaves > twigs ~ inner bark ~ branches ~ roots > outer bark ~ wood. In beeches investigated here, K concentration in outer bark is as high as that in inner bark and K concentration in branches as well as roots are not significantly different from that in wood. The variability between organs (excluding leaves) was contained within a factor of respectively 8 and 3 for birches and oaks. Contrary to most species (Meerts, 2002), decreasing K concentrations from heartwood to sapwood were specifically observed for chestnut (Colin-Belgrand et al., 1996) and beech (Penninckx et al., 2001; Boucher and Côté, 2002), the heartwood of which is atypical (Penninckx et al., 2001).

3.2.3. Cs-137 and stable analogues inventories

Beech is the common tree species for the 3 sites, allowing the analyse of the site effect. For sites comparison purpose, we normalized the Cs-137 inventories in beech trees by the site-specific basal area of beech trees (Table 1) to discard the influence of the varying beech abundances among sites. After normalization, beech vegetation accounted for respectively 0.3%, 1.5% and 0.5% of the total activity in HET, CPS and PS stands, respectively (Supp. Mat. Table S4.2), showing that soil remained by far the major reservoir of Cs-137 in the long-term after deposition. The beech vegetation of CPS stand accumulated a relatively higher proportion of Cs-137 *vs.* HET stand, while the deposition conditions were similar (global *vs.* Chornobyl fallouts). It is also the case *vs.* PS stand for which a higher accumulation would have been expected due to the main contribution of Chornobyl fallouts. In the monospecific birch and oak stands studied by Tsvetnova et al. (2018), the contributions of tree vegetation to the total Cs-137 inventory were 0.1% and 0.3%, respectively. In the deciduous broadleaf stands (*Q. serrata* Murray) investigated by Imamura et al. (2017) four years after the Fukushima accident, the contributions of tree vegetation (normalized by the basal area) ranged between 0.2 and 9.0% (N = 6). Such a wide range likely resulted from the variability of stand characteristics and atmospheric fallouts.

For Cs-133, tree vegetation contributed to respectively 0.02%, 0.1 % and 0.02% (normalized values) at HET, CPS and PS sites. The corresponding values for K are one order of magnitude higher than Cs-133 which might result in Cs discrimination by root absorption. Indeed, a factor of 10 is consistent with the values of the Cs *vs.* K discrimination factor measured by Zhu and Smolders (2000) in crops (values varying between 0.1 and 0.2). No obvious explanation could be set up for the higher relative accumulation of stable Cs by a factor 5 observed at CPS site.

The distribution of biomass between tree organs was the same in all stands (Fig. 5a). The partitioning of Cs isotopes was rather similar but differed from that of K (Fig. 5b,c,d). Roots were the main contributor for Cs isotopes but not for K, while stemwood was the main contributor to K inventory and biomass (Supp. Mat. table S4.4). Stemwood remained the second most important reservoir for Cs isotopes. For both stable Cs and K, heartwood contributed more than sapwood at the three sites. Cs also differed from K with respect to leaves, branches and, to less extent, bark. Twigs displayed the same lowest contribution for both elements (0.04–0.09%) because of its low biomass percentage (0.04%). An enhanced accumulation of Cs-137 in roots compared to shoots was already noticed by Fesenko et al. (2001a) for birch trees (*Betula pendula* Roth) and by von Fircks et al. (2002) for one-year-old willows (*Salix viminalis* L.) grown in short rotation coppice on contaminated arable soils. It argues that coarse roots are active for Cs-137 storage as observed in the case study. In the same experimental conditions and for the same species (von Fircks et al., 2002), Gommers et al. (2000) observed the lower accumulation for K in roots combined with the higher one for Cs-137. Gommers et al. (2000 and references therein) reported that hydroponically grown plants also accumulated radiocaesium in the roots and suggested that the xylem vessel may act as a second selective barrier to radiocaesium ascending to aboveground biomass (see also Fesenko et al., 2001a). From a physiological point of view, according to Ehlken and Kirchner (2002) the symplastic pathway is used to transport ions from roots to xylem parenchyma cells where they are released into the apoplasm of the xylem vessels. These authors suggested that the Cs/K discrimination of root uptake from soil solution (White and Broadley, 2000) were like those prevailing at the xylem entry. To our knowledge, Cs/K discrimination factors have mostly been addressed for crops grown in hydroponic conditions. Our results are consistent with the above-cited studies. An exception is the study of Kobayashi et al. (2019) dealing with Konara oak (*Q. serrata* Murray) seedlings grown in hydroponics under low K contents (50 μM), which demonstrated a higher discrimination of Cs by aboveground organs than (fine) roots.

3.3. Analysis of root transfer to tree vegetation

3.3.1. Aggregated transfer factor of Cs-137 for beeches (*Tag*)

To compare Cs-137 concentrations in tree organs between sites of varying atmospheric deposits (Table 1), we normalized them (Bq kg^{-1}) by the total activity inventory in the stand (Bq m^{-2}). As the contribution of tree vegetation to the inventory is negligible (<2%), the normalized concentrations correspond to the so-called aggregated transfer factor, denoted *Tag* (m^2 kg^{-1}), which quantifies the apparent transfer of radionuclides from soil to plants in semi-natural ecosystems (e.g. IAEA, 2010; Hashimoto et al., 2022). The *Tag* values (detailed in Supp. Mat. Table S5.1) can be compared with those of the literature on beech trees in Table 2.

The present *Tag* values rank as follows: leaves ≥ branches ~ stemwood. They are definitely lower than those published in the literature for beech trees. The *Tag*s also differ from those measured for other deciduous species more than a decade after Chornobyl accident (IAEA, 2009), i.e. lower for stemwood (0.1–3.8 10^{-3} m^2 kg^{-1} dw) and much lower for leaves (3–30 10^{-3} m^2 kg^{-1} dw). For birch and oak investigated 24 years after the Chornobyl accident by Tsvetnova et al. (2018), the *Tag* values were consistent with our data for leaves (around 0.1 10^{-3} m^2 kg^{-1} dw) but the data for stemwood were abnormally low compared with other studies (0.3–1 10^{-6} m^2 kg^{-1} dw), without any explanation being given by those authors. Based on post-Chornobyl studies, Ehlken and Kirchner (2002) suggested that *Tag*s would decrease with the years following deposition. This could explain why, in the current long-term field study, fairly low *Tag*s compared to previous ones were observed. Such temporal dependence seems to be confirmed by Vinichuk et al.

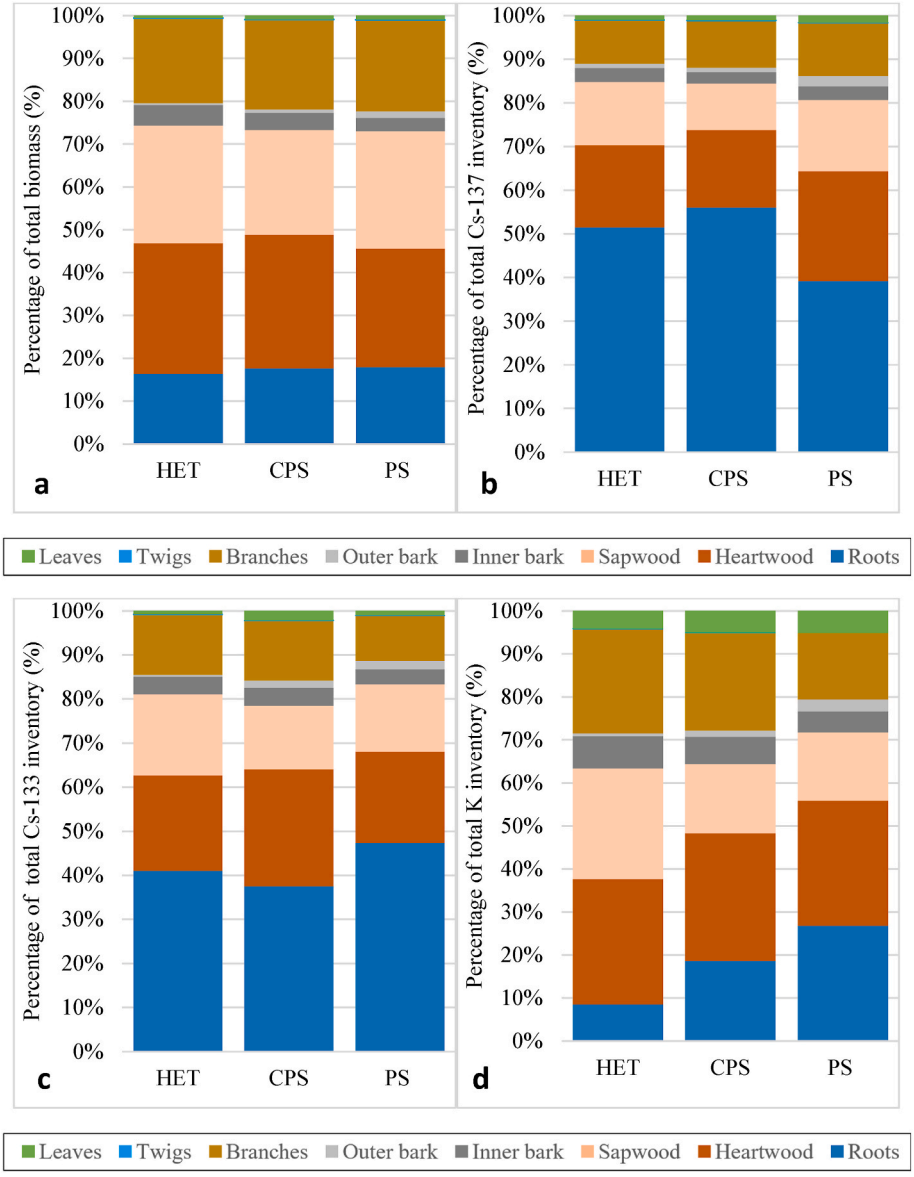

Fig. 5. (a) – Contribution of each beech tree organ to the total dry biomass. (b,c,d) – Contribution of each beech tree organ to the total inventory of Cs-137, Cs-133 and K, respectively.

Table 2
Aggregated transfer factor (Tag) of Cs-137 to beech organs measured in this study and in the literature.

Beech organs	*Tag* ($\times 10^{-3}$ m^2 kg^{-1} dw)	Sampling year	Reference
Leaves	*0.2–1.1*	*2021*	*This study*
	0.2–7.4	2001	Lamarque et al. (2005)
	2.3–2.7	1997	Belli (2000)
Branches	*0.06–0.4*	*2021*	*This study*
	0.2–5.2	2001	Lamarque et al. (2005)
Stemwood	*0.07–0.5*	*2021*	*This study*
	1.3–1.6	1997	Belli (2000)

(2023) who observed a decrease in *Tags* over the period 2012–2021 in sampled shoots of oak, ash (*Fraxinus* spp.) and rowan trees (*Sorbus* spp.) contaminated by Chornobyl fallouts. Nevertheless, due to the lack of long-term data, the temporal trend of Cs-137 *Tags* needs to be better documented.

Calmon et al. (2009) and references therein reported that soil parameters, mainly clay content, exchangeable K and time elapsed after deposition (Absalom et al., 1999, 2001; Ehlken and Kirchner, 2002), were the main factors explaining the variability of root transfer of Cs-137 in forest stands. The time effect (ageing) is attributed to the sorption of Cs-137 and its irreversible fixation on clays (Kruyts and Delvaux, 2002), which reduces its mobility in the soil (Bunzl et al., 1995a, 1995b). Several authors reported that the root transfer factor (TF = $[Cs\text{-}137]_{plant}/[Cs\text{-}137]_{soil}$ in Bq kg^{-1} dw/Bq kg^{-1} dw, dimensionless) was inversely proportional to the Radiocaesium Interception Potential (*RIP*), for both vascular plants (Smolders et al., 1997; Delvaux et al., 2000; Konopleva et al., 2009; Zibold et al., 2009) and trees (Gommers et al., 2000; Kruyts and Delvaux, 2002; Kruyts et al., 2004). The *RIP* parameter is an intrinsic soil parameter that characterizes the radiocaesium retention process in soil (Cremers et al., 1988; Sweeck et al., 1990; Wauters et al., 1996; Vandebroek et al., 2012). It can be estimated based on the sorption capacity of FES (Frayed Edges Sites) on the micas clay particles, which have a stronger affinity for Cs^+ compared to K^+. The selectivity of FES for Cs^+ is about 10^3 which is three orders of magnitude higher compared to the regular exchangeable complex. Thus,

the cationic composition of the soil solution (Cs^+ and K^+) and the abundance of FES are the factors determining Cs-137 retention in soil (Cremers et al., 1988; Wauters et al., 1996; Kruyts et al., 2004):

$$RIP = K_c^{FES} \times [FES] \quad (9)$$

Where *RIP* is the Radiocaesium Interception Potential (mmol kg^{-1}), K_c^{FES} is the selectivity coefficient in the FES for Cs-137/K and [*FES*] is the Frayed Edge Sites abundance (mmol kg^{-1}). Equation (9) is equivalent to Equation (10) (Wauters et al., 1996):

$$RIP = K_d^{Cs} \times [K^+]_{ss} \quad (10)$$

Where K_d^{Cs} is the solid-liquid distribution coefficient for radiocaesium (L kg^{-1}) and $[K^+]_{ss}$ is the concentration of K^+ in soil solution (mmol L^{-1}).

We attempted to estimate *RIP* values for HET, CPS and PS sites from the meta-analysis of Vandebroek et al. (2012), by deriving a linear regression between Cs-137 exchangeable fractions measured by NH_4Ac and HCl extractions (according to soil type, cambisol: pearson's r = 0.9, p-value <0.001, podzol: pearson's r = 0.8, p-value <0.05), then using the linear model between *RIP* and the exchangeable fraction based on HCl extraction. The estimated *RIP* differed by 2 orders of magnitude between HET (14000 mmol kg^{-1}) and CPS/PS sites (200 and 160 mmol kg^{-1}, respectively). Even if the nature of clay quantitatively influences their sorption capacity of Cs (e.g. vermiculite > kaolinite, cf. Nakao et al., 2008), such a difference between cambisol and podzol soils was expected due to their contrasted clay contents (cf. Table 1) which strongly influences FES abundance (Delvaux et al., 2000; Vandebroek et al., 2012). Indeed, a higher clay content in HET soil likely explains lower *Tags* in aboveground biomass: 6.5 10^{-5} m^2 kg^{-1} at HET site *vs* 2.6/4.9 10^{-4} m^2 kg^{-1} at CPS/PS sites. However, the absence of significant difference between *RIP*s at CPS and PS could hardly explain the *Tags* difference by a factor 2. The Cs-137 exchangeable fraction was twice higher for PS than CPS (Supp. Mat. Table S4.1) and may be related to the twice higher CEC in soil mineral horizon of PS vs. CPS, but also to the shorter delay from deposition. Soil parameters could also constitute another source of variability: clay mineralogy (Vandebroek et al., 2012; Hashimoto et al., 2022), soil pH (Gandois et al., 2010; De Tombeur et al., 2020) and other competing cations in the soil solution (NH_4^+, Na^+, Ca^{2+}, Mg^{2+}) involved in the solid-liquid exchange with the clay-humic complex (cf. Smolders et al., 1997; Konopleva et al., 2009).

3.3.2. *Normalized concentrations of Cs-137 and stable analogues in beeches (NCE)*

The exchangeable fractions of Cs-137, Cs-133 and K in soil, resulting from complex biophysiochemical processes taking place in the rooting layers, were considered as the bioavailable pools from which root uptake occurred. Normalizing concentrations in tree organs by the

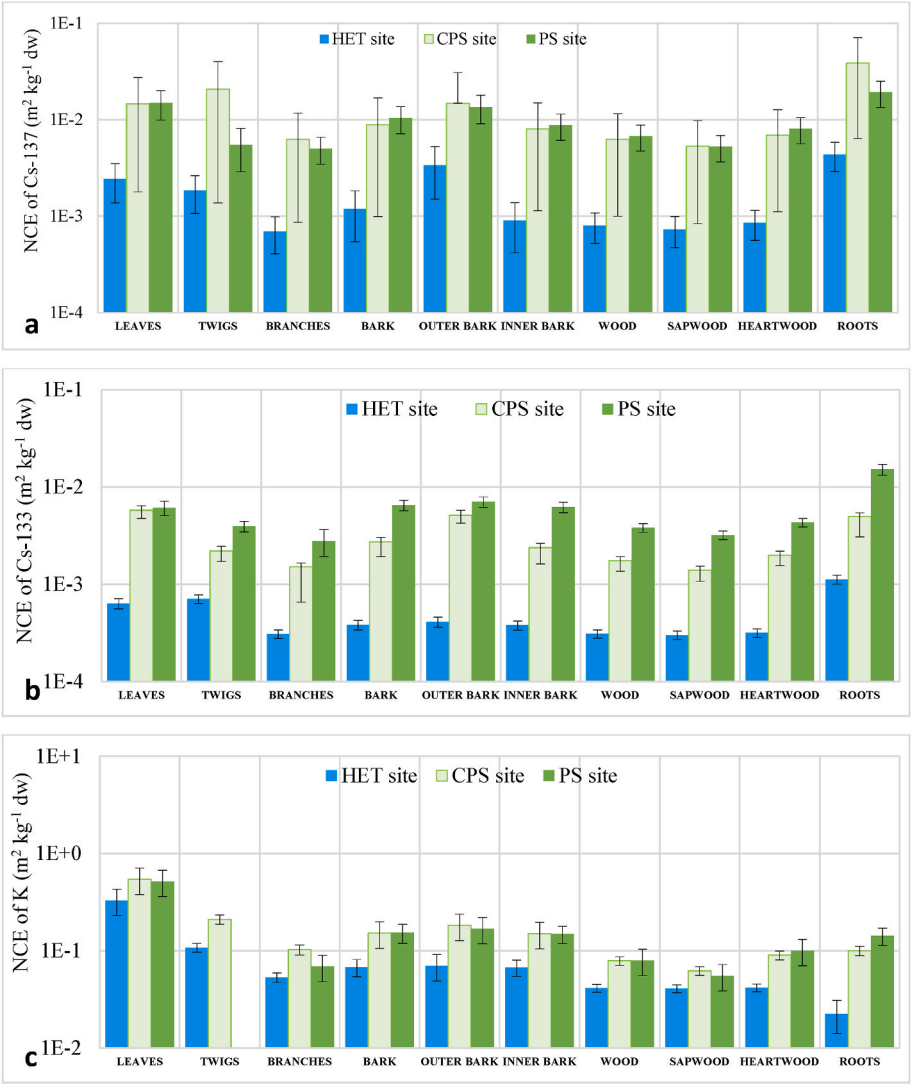

Fig. 6. (a,b,c) – NCE of Cs-137, Cs-133 and K in beech tree organs, respectively. Error bars correspond to 1 standard deviation.

exchangeable inventory instead of the total inventory in the 0–40 cm mineral layer (*NCE* – Normalized Concentration by the Exchangeable inventory) contributed to reduce the variability of the soil-to-tree transfer factors (Thørring et al., 2012; Kanasashi et al., 2020; Yoschenko et al., 2022). Since the structural pool contributes most to soil Cs-133 and K contents, the use of *NCE*s instead of *Tag*s provides better information on the true extent of the uptake process at each site. The *NCE* values in tree organs are displayed in Fig. 6 (Supp. Mat. Table S5.2). They were systematically lower at HET site than at the CPS and PS sites: a difference of about one order of magnitude for Cs-137, a factor of 5–10 for Cs-133 and from 2 to 6 for K (Supp. Mat. Table S5.3). For Cs-137 and K, the CPS and PS sites were not significantly different. For Cs-133, *NCE*s were generally lower at the CPS site than at the PS site (by nearly a factor of almost 2). With regards to the variability between elements and isotopes, the *NCE*s of K were much higher than those for Cs, by one to two orders of magnitude depending on the isotope and site considered (Supp. Mat. Table S5.4). Regarding the difference between Cs isotopes, we note that the *NCE*s of Cs-137 were generally a factor of 3 higher than the *NCE*s of Cs-133, the largest difference being for beech roots at the CPS site, i.e. a factor of 8.

We expected that the normalization of concentrations by the exchangeable inventory in the 0–40 cm mineral soil would have decreased the variability of transfer factors between sites. This is definitely not the case since there remains up to one order of magnitude difference between cambisol and podzol sites, particularly for caesium isotopes. This suggests that other factors than the total deposit (for Cs-137) and the exchangeable fraction (such as measured in this study) play a role in the intake of elements by tree organs. Other factors of variability are addressed in the next section.

3.3.3. *Relationships between normalized concentrations of Cs-137 and stable analogues in beeches*

The relationship between Cs-137 and Cs-133 normalized concentrations in tree organs was examined and best illustrated by a linear regression model without intercept, i.e. *NCE* Cs-137 = a × *NCE* Cs-133 before Log transformation (Fig. 7a, see Supp. Mat. Table S6.1 for pearson's r values and attached p-values). This best fit was obtained by minimizing the RMSLE of *NCE*s or equivalently, maximizing the coefficient of determination (r^2) based on the log-values of *NCE*s. As Fig. 7a shows, the normalized concentration of Cs-137 was predicted fairly well by that of Cs-133 when the three sites were grouped together ($r^2 = 0.80$; n = 98, p-value < 1E-07), whereas it was less convincing for the podzol sites dataset ($r^2 = 0.38$; n = 44, p-value = 5.0 E−07) because of the noticeable scattering between PS and CPS data points. When considered separately, these two sites were much better fitted by the linear model ($r^2 = 0.75$ and 0.86 for respectively CPS and PS, n = 22, p-values < 1E-07). The absence of intercept seems to confirm that the contribution of foliar uptake of airborne Cs-137 at the time of atmospheric fallouts is no longer visible in the long-term. This implies that, after decades of recycling of radioactivity in the soil-tree system, the distribution of Cs-137 is now mainly determined by root uptake, internal translocations in tree vegetation and transfer fluxes back to the soil.

The linear regression slope inferred from Fig. 7a for the complete Cs-137 vs Cs-133 dataset was ~3, which value was in close agreement with those established separately for the cambisol and podzol sites. Turning back to the semi-mechanistic modelling approach described in paragraph 2.5, it is worth examining to what extent the slope predicted by Equation (9) was consistent with the value observed. For mineral soils with bulk densities slowly increasing with depth, one can check that the multiplying factor (quantifying the heterogeneity of mainly root density and Cs-137 profiles in the rooting zone) is close to 1 if either root density or Cs-137 concentration do not much vary with depth. On the contrary, if the two profiles are strongly inhomogeneous, this slope becomes significantly greater than 1 when these two variables are positively correlated (e.g. they both decrease with depth) or significantly smaller than 1 when negatively correlated. Generally, the density of fine active roots decreases with depth and is maximum in the upper mineral soil layers where nutrients leached from the organic layers accumulate. As exchangeable Cs-137 inventory also decreased with depth at the studied sites (cf. Fig. 2b), one might expect a slope greater than 1. This point could be checked quantitatively, based on the measured Cs-137 and soil density profiles down to z = 40 cm depth (see Supp. Mat. Table S4.1), plus one additional hypothesis regarding the fine root density profile (not measured). If one assumes an exponential root density profile, it can be verified that this slope increases to a mean value consistent with Fig. 7a as long as root density decreases with depth according to α_j^{up} coefficients equal to respectively 0.95 and 0.05 in the 0–10 cm and 10–20 cm mineral layers (95% of the fine root biomass is contained within the top 10 cm mineral soil), fine root biomass abundance being negligible in the 20–40 cm layer. Such a distribution which corresponds to the following truncated exponential profile: $\rho(z) = 0.3\ cm^{-1} \times \exp$

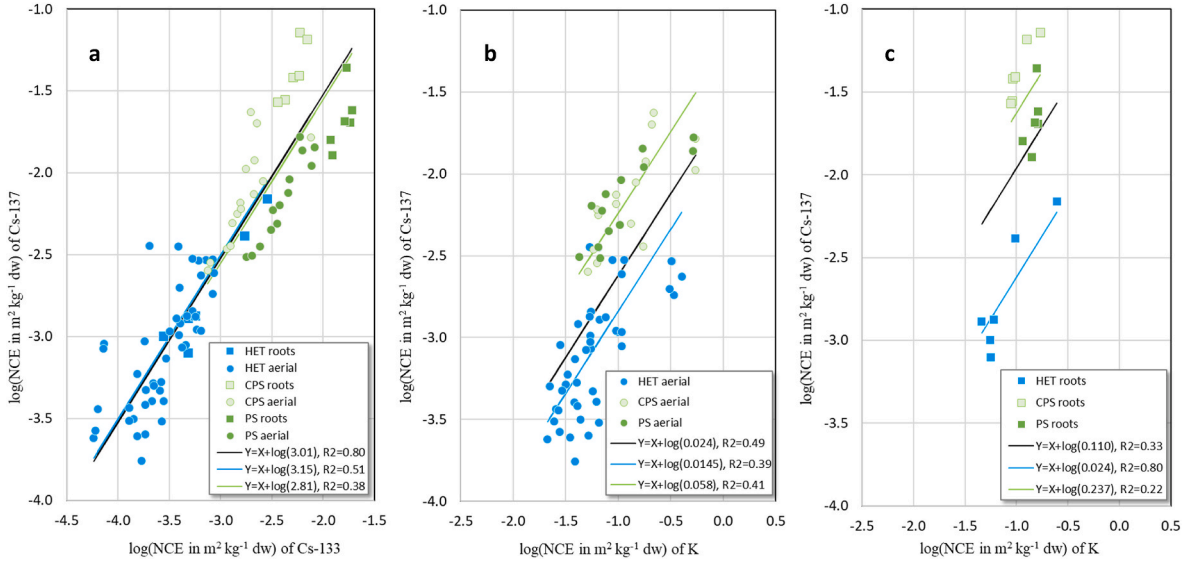

Fig. 7. (a,b,c) – Relationships between NCEs of Cs-137 vs. Cs-133, NCEs of Cs-137 vs. K in aerial organs and in roots, respectively. Lines represent the best fitted linear relationships established for all sites together (black line), HET cambisol site (blue line) and CPS/PS podzol sites (green line). (For interpretation of the references to colour in this figure legend, the reader is referred to the Web version of this article.)

($-0.3\ cm^{-1} \times z$) for $z \leq 40$ cm, 0 cm^{-1} below, is plausible.

Regarding the linear relationship between Cs-137 and K normalized concentrations, we distinguished aerial organs from roots because we did not expect the same results (cf. paragraph 2.5). For aerial organs (Fig. 7b), the fit of the regression model was less satisfactory than for stable caesium, with r^2 values varying from 0.39 to 0.49 (all p-values <5.0 E−03) depending on the sites considered. This is mainly because the range of variability of K concentrations between organs and sites extends here over 1.5 order of magnitude compared with 2.5 for Cs-133, while the range of variability of Cs-137 concentrations at a given stable concentration does not much change. This mechanically decreases the value of r^2. As depicted in Fig. 7b, the estimated slope for grouped sites was slightly less than 0.025, which value was much smaller than for Cs-133. There was also a striking difference between the cambisol and podzol sites, with regression slopes differing by a factor 4, i.e. 0.0145 for cambisol site (HET) against 0.058 for podzol sites (CPS + PS). Regarding root organs for which data are rather sparse (Fig. 7c) and the range of K concentrations are even narrower than for aerial organs, the relevance of the linear regression model could not be demonstrated, even though Cs-137 and K concentrations were positively correlated at HET and CPS sites (see Supp. Mat. Table S6.1). Under the hypothesis of linearity, the estimated slopes appear greater than those estimated in aerial organs, i.e. by a factor of 2–4 depending on sites. Although very uncertain, it would suggest some discrimination effect in internal translocation processes (see below).

As long *in-situ* measurements are robust and the linear model is validated, it is possible to estimate selectivity coefficients by comparing slopes obtained for Cs-137/K and Cs-137/Cs-133 relationships (cf. paragraph 2.5). Focusing on aerial organs, for which these two conditions are met, enables to evaluate the net selectivity coefficient. If we assume that it only depends on tree species but not on sites (i.e. soil, climate characteristics), we estimated $sel^{tra} \times sel^{up} \sim 0.008$ for aerial organs. Such a value was unexpected because it is surprisingly low compared to those estimated for the shoots of crops grown in hydroponics conditions on the short term, which typically vary between 0.1 and 0.2 (e.g. Zhu and Smolders, 2000; Casadesus et al., 2008). The situations however are very different as we are dealing here with tree plants grown on forest soils and long-term measurements. By comparing Cs-137/K concentration ratios measured in aerial organs and roots, one can further identify whether there is a discrimination by internal translocation processes between Cs-137 and K. If so, concentration ratios in aerial organs, notably foliage, would be smaller than in roots. Despite a strong variability between sites or organs, this seems confirmed by our data (Fig. 4) from which we derived the following values for average Cs-137/K ratios: ~1.8 Bq g^{-1} K in roots against ~0.32 Bq g^{-1} K in aerial organs (~0.15 Bq g^{-1} K in leaves). This would suggest a mean value sel^{tra} ~0.18 (0.32 Bq g^{-1} K/1.8 Bq g^{-1} K). Despite the fact that slope estimates for roots are not very reliable, we nevertheless inferred selectivity coefficients specific to each transfer process by comparing root and shoot slopes, which led to the following values: sel^{up} ~0.037 and sel^{tra} ~0.22. We notice that the value obtained for translocation is rather consistent with that deduced above from Cs-137/K concentration ratios. These results would suggest that discrimination is much more effective during root uptake than translocation to above-ground parts.

These above results must be treated with some caution because they are based on the hypothesis of an analogy between Cs-137 and K, which is not fully confirmed by the observations. Furthermore, the model described above assumes that root uptake is the only supplier of chemical elements to growing trees organs and does not consider internal (re)translocations between aerial organs, or return-to-soil loss fluxes, which could also be subject to Cs/K discrimination according to the physiological pathway. However, the magnitude of internal translocations is a supplementary source of variability between sites because these processes depend on the soil capacity to supply nutrients required for plant growth (Legout et al., 2020). Another point is that the contribution of organic soil was not accounted for in the study when estimating *NCEs*, although it also contributes to the transfer of Cs-137 and stable analogues to tree vegetation. Indeed, Of and Oh layers are colonised by roots and have been shown to have low *RIP* values due to low amounts of FES (Kruyts and Delvaux, 2002). Finally, we know from Bel et al. (2020) that the inventory of bioavailable K in soil is underestimated by conventional extraction analyses, meaning a higher bioavailable pool of K than estimated in our study. This is another source of uncertainty in the results or variability between sites.

4. Conclusion

As expected in the long-term, the mineral soil horizon is the major reservoir of the Cs-137 deposits and at least 80% of its inventory is found in the 0–20 cm mineral layers whatever the site. The initial interception of Cs-137 deposit and subsequent internalization through foliar uptake pathway is no more visible in beech organs and equilibrium was reached within stands compartments. In this steady state context, Cs-133 appears a better chemical analogue of Cs-137 than K to address its root uptake if considering the tree root density according to depth to define the rooting zone, i.e. the relevant soil layer to account for. Focusing on a single tree species, this study allowed identifying site effects, notably soil parameters driving the root uptake intensity of Cs-137.

Long-term scale effects are visible through the decrease of Cs-137 *Tags* in trees aboveground organs and the significant accumulation of this radioisotope in roots. Slow processes as root uptake increased the variability between sites. In this respect, internal translocations probably amplified the variability between tree species leading the deciduous species appearing a less homogenous group than assumed. Since they don't account for eco-physiological and geochemical processes, the modelling approaches relying on aggregated transfer factors (*Tags*) are limited to encompass the observed variability over time. The use of models relying on the biogeochemical cycle would better address the Cs-137 dynamic in forest, provided that specific dataset is available.

CRediT authorship contribution statement

D. Okhrimchuk: Writing – original draft, Investigation, Visualization. **P. Hurtevent:** Writing – original draft, Conceptualization, Investigation, Writing – review & editing. **M.-A. Gonze:** Writing – original draft, Conceptualization, Investigation, Writing – review & editing. **M. Simon-Cornu:** Supervision, Project administration, Writing – review & editing. **M. Roulier:** Investigation, Writing – review & editing. **L. Carasco:** Investigation, Resources. **D. Orjollet:** Resources, Validation. **M. Nicolas:** Resources, Validation, Writing – review & editing. **A. Probst:** Writing – original draft, Supervision.

Declaration of competing interest

The authors declare that they have no known competing financial interests or personal relationships that could have appeared to influence the work reported in this paper.

Data availability

Data will be made available on request.

Acknowledgements

We are grateful to C. Devedeux, V. Lange and T. Lavaupot from ONF for their welcoming on the RENECOFOR plots and the logistic help they provided for the field sampling campaigns. We also thank G. Salaün and D. Mourier from IRSN/PSE-ENV for their valuable help during field sampling and samples treatment.

Appendix A. Supplementary data

Supplementary data to this article can be found online at https://doi.org/10.1016/j.jenvrad.2024.107450.

References

Absalom, J.P., Young, S.D., Crout, N.M.J., Nisbet, A.F., Woodman, R.F.M., Smolders, E., Gillett, A.G., 1999. Predicting soil to plant transfer of radiocesium using soil characteristics. Environ. Sci. Technol. 33, 1218–1223. https://doi.org/10.1021/es9808853.

Absalom, J.P., Young, S.D., Crout, N.M.J., Sanchez, A., Wright, S.M., Smolders, E., Nisbet, A.F., Gillett, A.G., 2001. Predicting the transfer of radiocaesium from organic soils to plants using soil characteristics. J. Environ. Radioact. 52, 31–43. https://doi.org/10.1016/S0265-931X(00)00098-9.

Baeza, A., Guillén, J., Espinosa, A., Aragón, A., Gutierrez, J., 2005. A study of the bioavailability of ^{90}Sr, ^{137}Cs, and $^{239+240}$Pu in soils at two locations of Spain affected by different radionuclide contamination events. Radioprotection 40, S61–S65. https://doi.org/10.1051/radiopro:2005s1-010.

Bartelink, H., 1997. Allometric relationships for biomass and leaf area of beech (Fagus sylvatica L.). Ann. For. Sci. 54, 39–50. https://doi.org/10.1051/forest:19970104.

Bel, J., Legout, A., Saint-André, L., Hall, S.J., Löfgren, S., Laclau, J.-P., van der Heijden, G., 2020. Conventional analysis methods underestimate the plant-available pools of calcium, magnesium and potassium in forest soils. Sci. Rep. 10, 15703 https://doi.org/10.1038/s41598-020-72741-w.

Belli, M., 2000. Long-term dynamics of radionuclides in semi-natural environments: derivation of parameters and modelling. Rome, Italy. In: Belli, M. (Ed.), Final Report 1996-1999. Report ANPA-RT–00-010, p. 105. ISBN 88-448-0286-4.

Berg, M.T., Shuman, L.J., 1995. A three-dimensional stochastic model of the behavior of radionuclides in forests III. Cs-137 uptake and release by vegetation. Ecol. Model. 83, 387–404. https://doi.org/10.1016/0304-3800(94)00105-5.

Boucher, P., Côté, B., 2002. Characterizing base-cation immobilization in the stem of six hardwoods of eastern Canada. Ann. For. Sci 59, 397–407. https://doi.org/10.1051/forest:2002014.

Brêthes, A., Ulrich, E., 1997. RENECOFOR - Caractéristiques pédologiques des 102 peuplements du réseau. ONF (Office National des Forêts). Fontainebleau, France, p. 573 in French. ISBN 978-2-84207-112-7. https://appgeodb.nancy.inra.fr/biljou/pdf/Brethes_et_al_1997_Description_sols.pdf.

Bunzl, K., Schimmack, W., Kreutzer, K., Schierl, R., 1989. Interception and retention of chernobyl-derived ^{134}Cs, ^{137}Cs and ^{106}Ru in a spruce stand. Sci. Total Environ. 78, 77–87. https://doi.org/10.1016/0048-9697(89)90023-5.

Bunzl, K., Kracke, W., Schimmack, W., Auerswald, K., 1995a. Migration of fallout $^{239+240}$Pu, ^{241}Am and ^{137}Cs in the various horizons of a forest soil under pine. J. Environ. Radioact. 28, 17–34. https://doi.org/10.1016/0265-931X(94)00066-6.

Bunzl, K., Schimmack, W., Krouglov, S.V., Alexakhin, R.M., 1995b. Changes with time in the migration of radiocesium in the soil, as observed near Chernobyl and in Germany, 1986–1994. Sci. Total Environ. 175, 49–56. https://doi.org/10.1016/0048-9697(95)04842-1.

Burger, A., Lichtscheidl, I., 2018. Stable and radioactive cesium: a review about distribution in the environment, uptake and translocation in plants, plant reactions and plants' potential for bioremediation. Sci. Total Environ. 618, 1459–1485. https://doi.org/10.1016/j.scitotenv.2017.09.298.

Calmon, P., Thiry, Y., Zibold, G., Rantavaara, A., Fesenko, S., 2009. Transfer parameter values in temperate forest ecosystems: a review. J. Environ. Radioact. 100, 757–766. https://doi.org/10.1016/j.jenvrad.2008.11.005.

Calvaruso, C., Kirchen, G., Saint-André, L., Redon, P.-O., Turpault, M.-P., 2017. Relationship between soil nutritive resources and the growth and mineral nutrition of a beech (Fagus sylvatica) stand along a soil sequence. Catena 155, 156–169. https://doi.org/10.1016/j.catena.2017.03.013.

Casadesus, J., Sauras-Yera, T., Vallejo, V.R., 2008. Predicting soil-to-plant transfer of radionuclides with a mechanistic model (BioRUR). J. Environ. Radioact. 99, 864–871. https://doi.org/10.1016/j.jenvrad.2007.10.013.

Chakraborty, T., Saha, S., Reif, A., 2016. Biomass equations for European beech growing on dry sites. iFor. Biogeosci. For. 9, 751–757. https://doi.org/10.3832/ifor1881-009.

Clouvas, A., Xanthos, S., Takoudis, G., Antonopoulos-Domis, M., Alifrangis, D.A., Zhiyanski, M., Sokolovska, M., 2007. Following up study of radiocesium contamination in a Greek forest ecosystem. Health Phys. 93, 312–317. https://doi.org/10.1097/01.hp.0000266738.48868.17.

Colin-Belgrand, M., Ranger, J., Bouchon, J., 1996. Internal nutrient translocation in chestnut tree stemwood: III. Dynamics across an age series of Castanea sativa (Miller). Ann. Bot. 78, 729–740. https://doi.org/10.1006/anbo.1996.0183.

Coppin, F., Hurtevent, P., Loffredo, N., Simonucci, C., Julien, A., Gonze, M.-A., Nanba, K., Onda, Y., Thiry, Y., 2016. Radiocaesium partitioning in Japanese cedar forests following the "early" phase of Fukushima fallout redistribution. Sci. Rep. 6, 1–11. https://doi.org/10.1038/srep37618.

Cremers, A., Elsen, A., Preter, P.D., Maes, A., 1988. Quantitative analysis of radiocaesium retention in soils. Nature 335, 247–249. https://doi.org/10.1038/335247a0.

Delvaux, B., Kruyts, N., Cremers, A., 2000. Rhizospheric mobilization of radiocesium in soils. Environ. Sci. Technol. 34, 1489–1493. https://doi.org/10.1021/es990658g.

Devillez, F., Jain, T.C., Marynen, T., Iserentant, R., Jouret, M.F., Lebrun, J., Renard, Ch, 1973. Structure et biomasse d'une hêtraie en Haute-Ardenne. Bull. Académie R. Belg 303–331. https://www.persee.fr/doc/barb_0001-4141_1973_num_59_1_60698. last accessed 2023.02.12.

De Tombeur, F., Cornu, S., Bourlès, D., Duvivier, A., Pupier, J., Team, A.S.T.E.R., Brossard, M., Evrard, O., 2020. Retention of ^{10}Be, ^{137}Cs and ^{210}Pb$_{xs}$ in soils: impact of physico-chemical characteristics. Geoderma 367, 114242. https://doi.org/10.1016/j.geoderma.2020.114242.

Ehlken, S., Kirchner, G., 2002. Environmental processes affecting plant root uptake of radioactive trace elements and variability of transfer factor data: a review. Radionucl. Soil-Plant Syst. 58, 97–112. https://doi.org/10.1016/S0265-931X(01)00060-1.

Evrard, O., Laceby, J.P., Lepage, H., Onda, Y., Verdan, O., Ayrault, S., 2015. Radiocesium transfer from hillslopes to the pacific ocean after the Fukushima nuclear power plant accident: a review. J. Environ. Radioact. 148, 92–110. https://doi.org/10.1016/j.jenvrad.2015.06.018.

Fesenko, S.V., Soukhova, N.V., Sanzharova, N.I., Avila, R., Spiridonov, S.I., Klein, D., Lucot, E., Badot, P.M., 2001a. Identification of processes governing long-term accumulation of ^{137}Cs by forest trees following the Chernobyl accident. Radiat. Environ. Biophys. 40, 105–113. https://doi.org/10.1007/s004110100090.

Fesenko, S.V., Soukhova, N.V., Sanzharova, N.I., Avila, R., Spiridonov, S.I., Klein, D., Badot, P.-M., 2001b. ^{137}Cs availability for soil to understory transfer in different types of forest ecosystems. Sci. Total Environ. 269, 87–103. https://doi.org/10.1016/S0048-9697(00)00818-4.

Fesenko, S., Sukhova, N., Spiridonov, S., Sanzharova, N.I., Avila, R., Klein, D., Badot, P. M., 2003. Distribution of 137Cs in the tree layer of forest ecosystems in the zone of the accident at the chernobyl nuclear power plant. Russ. J. Ecol. 34, 104–109. https://doi.org/10.1023/A:1023047030350.

Fogh, C.L., Andersson, K.G., 2001. Dynamic behaviour of ^{137}Cs contamination in trees of the Briansk region, Russia. Sci. Total Environ. 269, 105–115. https://doi.org/10.1016/S0048-9697(00)00819-6.

Gandois, L., Probst, A., Dumas, C., 2010. Modelling trace metal extractability and solubility in French forest soils by using soil properties. Eur. J. Soil Sci. 61, 271–286. https://doi.org/10.1111/j.1365-2389.2009.01215.x.

Genet, A., Wernsdörfer, H., Jonard, M., Pretzsch, H., Rauch, M., Ponette, Q., Nys, C., Legout, A., Ranger, J., Vallet, P., Saint-André, L., 2011. Ontogeny partly explains the apparent heterogeneity of published biomass equations for Fagus sylvatica in central Europe. For. Ecol. Manag. 261, 1188–1202. https://doi.org/10.1016/j.foreco.2010.12.034.

Gommers, A., Thiry, Y., Vandenhove, H., Vandecasteele, C.M., Smolders, E., Merckx, R., 2000. Radiocesium uptake by one-year-old willows planted as short rotation coppice. J. Environ. Qual. 29, 1384–1390. https://doi.org/10.2134/jeq2000.00472425002900050003x.

Gonze, M.-A., Calmon, P., 2017. Meta-analysis of radiocesium contamination data in Japanese forest trees over the period 2011–2013. Sci. Total Environ. 601–602, 301–316. https://doi.org/10.1016/j.scitotenv.2017.05.175.

Gonze, M.-A., Calmon, P., Hurtevent, P., Coppin, F., 2021. Meta-analysis of radiocesium contamination data in Japanese cedar and cypress forests over the period 2011–2017. Sci. Total Environ. 750, 142311 https://doi.org/10.1016/j.scitotenv.2020.142311.

Goor, F., Thiry, Y., 2004. Processes, dynamics and modelling of radiocaesium cycling in a chronosequence of Chernobyl-contaminated Scots pine (Pinus sylvestris L.) plantations. Sci. Total Environ. 325, 163–180. https://doi.org/10.1016/j.scitotenv.2003.10.037.

Hashimoto, S., Tanaka, T., Komatsu, M., Gonze, M.-A., Sakashita, W., Kurikami, H., Nishina, K., Ota, M., Ohashi, S., Calmon, P., Coppin, F., Imamura, N., Hayashi, S., Hirai, K., Hurtevent, P., Koarashi, J., Manaka, T., Miura, S., Shinomiya, Y., Shaw, G., Thiry, Y., 2021. Dynamics of radiocaesium within forests in Fukushima—results and analysis of a model inter-comparison. J. Environ. Radioact. 238–239, 106721 https://doi.org/10.1016/j.jenvrad.2021.106721.

Hashimoto, S., Komatsu, M., Miura, S., 2022. Behavior of radiocesium in the forest. In: Hashimoto, S., Komatsu, M., Miura, S. (Eds.), Forest Radioecology in Fukushima: Radiocesium Dynamics, Impact, and Future. Springer Nature, Singapore, pp. 21–46. https://doi.org/10.1007/978-981-16-9404-2_3.

Heinze, S., Ludwig, B., Piepho, H.-P., Mikutta, R., Don, A., Wordell-Dietrich, P., Helfrich, M., Hertel, D., Leuschner, C., Kirfel, K., Kandeler, E., Preusser, S., Guggenberger, G., Leinemann, T., Marschner, B., 2018. Factors controlling the variability of organic matter in the top- and subsoil of a sandy Dystric Cambisol under beech forest. Geoderma 311, 37–44. https://doi.org/10.1016/j.geoderma.2017.09.028.

Holiaka, D., Yoschenko, V., Cherniaiev, O.R., Moskaliuk, A., Lesnik, O., Levchuk, S., Holiaka, M., Gumenuk, V., Y. Kovbasa, Y., Borsuk, O., Holik, V., Nanba, K., Kashparov, V., 2023. Variability of activity concentrations and radial distributions of 137Cs and 90Sr in trunk wood of Scots pine and Silver birch. J. Environ. Radioact. 263, 107186 https://doi.org/10.1016/j.jenvrad.2023.107186.

IAEA, 2009. Quantification of radionuclide transfer in terrestrial and freshwater environments for radiological assessments. IAEA ed., Vienna, Austria TECDOC Series 1616 616. ISBN 978–92–0–104509–6.

IAEA, 2010. Handbook of parameter values for the prediction of radionuclide transfer in terrestrial and freshwater environment. IAEA ed., Vienna, Austria. In: Technical Report Series 472, p. 194. ISBN 978–92–0–113009–9.

Imamura, N., Komatsu, M., Ohashi, S., Hashimoto, S., Kajimoto, T., Kaneko, S., Takano, T., 2017. Temporal changes in the radiocesium distribution in forests over the five years after the Fukushima Daiichi Nuclear Power Plant accident. Sci. Rep. 7, 1–11. https://doi.org/10.1038/s41598-017-08261-x.

IRSN, 2015, IRSN ed.. Les retombées en France des essais nucléaires atmosphériques – Les retombées au sol. Fiche information 5.0 in French. https://www.irsn.fr/sites/default/files/documents/connaissances/environnement/retombees-tirs-armes-nucleaires/IRSN_serie_fiches_tirs_08-2015.pdf. (Accessed 15 November 2022).

IRSN, 2022. Le bruit de fond des radionucléides artificiels dans l'environnement français métropolitain bilan des constats radiologiques régionaux. Report IRSN/DG 2022-00131, IRSN ed. Fontenay-Aux-Roses, France, p. 152. in French. https://www.irsn.fr/rapport-dexpertise/bruit-fond-radionucleides-artificiels-dans-lenvironnement-francais-metropolitain. (Accessed 15 November 2022).

IUSS Working Group WRB, 2015. World Reference Base for Soil Resources 2014, Update 2015. International Soil Classification System for Naming Soils and Creating Legends for Soil Maps. World Soil Resources Reports No. 106. FAO, Rome, Italy. ISBN 978-92-5-108369-7.

Jagercikova, M., Cornu, S., Le Bas, C., Evrard, O., 2015. Vertical distributions of ^{137}Cs in soils: a meta-analysis. J. Soils Sediments 15, 81–95. https://doi.org/10.1007/s11368-014-0982-5.

Jagercikova, M., Cornu, S., Bourlès, D., Evrard, O., Hatté, C., Balesdent, J., 2017. Quantification of vertical solid matter transfers in soils during pedogenesis by a multi-tracer approach. J. Soils Sediments 17, 408–422. https://doi.org/10.1007/s11368-016-1560-9.

Jonard, M., Nicolas, M., Coomes, D.A., Caignet, I., Saenger, A., Ponette, Q., 2017. Forest soils in France are sequestering substantial amounts of carbon. Sci. Total Environ. 574, 616–628. https://doi.org/10.1016/j.scitotenv.2016.09.028.

Kanasashi, T., Miura, S., Hirai, K., Nagakura, J., Itô, H., 2020. Relationship between the activity concentration of ^{137}Cs in the growing shoots of Quercus serrata and soil 137Cs, exchangeable cations, and pH in Fukushima, Japan. J. Environ. Radioact. 220–221, 106276 https://doi.org/10.1016/j.jenvrad.2020.106276.

Karroum, M., Guillet, B., Laggoun-Défarge, F., Disnar, J.-R., Lottier, N., Villemin, G., Toutain, F., 2005. Evolution morphologique des litières de hêtre (Fagus sylvatica L.) et transformation des biopolymères, lignine et polysaccharides, dans un mull et un moder, sous climat tempéré (forêt de Fougères, Bretagne, France). Can. J. Soil Sci. 85, 405–416. https://doi.org/10.4141/S03-021 in French.

Kato, H., Onda, Y., Saidin, Z.H., Sakashita, W., Hisadome, K., Loffredo, N., 2019. Six-year monitoring study of radiocesium transfer in forest environments following the Fukushima nuclear power plant accident. J. Environ. Radioact. 210, 105817 https://doi.org/10.1016/j.jenvrad.2018.09.015.

Koarashi, J., Nishimura, S., Nakanishi, T., Atarashi-Andoh, M., Takeuchi, E., Muto, K., 2016. Post-deposition early-phase migration and retention behavior of radiocesium in a litter–mineral soil system in a Japanese deciduous forest affected by the Fukushima nuclear accident. Chemosphere 165, 335–341. https://doi.org/10.1016/j.chemosphere.2016.09.043.

Koarashi, J., Atarashi-Andoh, M., Nishimura, S., 2023. Effect of soil organic matter on the fate of ^{137}Cs vertical distribution in forest soils. Ecotoxicol. Environ. Saf. 262, 115177 https://doi.org/10.1016/j.ecoenv.2023.115177.

Kobayashi, R., Kobayashi, N.I., Tanoi, K., Masumori, M., Tange, T., 2019. Potassium supply reduces cesium uptake in Konara oak not by an alteration of uptake mechanism, but by the uptake competition between the ions. J. Environ. Radioact. 208–209, 106032 https://doi.org/10.1016/j.jenvrad.2019.106032.

Komatsu, M., Kaneko, S., Ohashi, S., Kuroda, K., Sano, T., Ikeda, S., Saito, S., Yoshiyuki Kiyono, Y., Tonosaki, M., Satoru Miura, S., Akama, A., Kajimoto, T., Takahashi, M., 2016. Characteristics of initial deposition and behavior of radiocesium in forest ecosystems of different locations and species affected by the Fukushima Daiichi Nuclear Power Plant accident. J. Environ. Radioact. 161, 2–10. https://doi.org/10.1016/j.jenvrad.2015.09.016.

Konopleva, I., Klemt, E., Konoplev, A., Zibold, G., 2009. Migration and bioavailability of ^{137}Cs in forest soil of southern Germany. J. Environ. Radioact. 100, 315–321. https://doi.org/10.1016/j.jenvrad.2008.12.010.

Krasnov, V.P., 1999. The direction and intensity of 137Cs fluxes in forest ecosystems. In: Linkov, I., Schell, W.R. (Eds.), Contaminated Forests: Recent Developments in Risk Identification and Future Perspectives, NATO Science Series, vol. 58. Springer, Dordrecht, Netherlands, pp. 71–76. https://doi.org/10.1007/978-94-011-4694-4_7.

Kruyts, N., Delvaux, B., 2002. Soil organic horizons as a major source for radiocesium biorecycling in forest ecosystems. J. Environ. Radioact. 58, 175–190. https://doi.org/10.1016/S0265-931X(01)00065-0.

Kruyts, N., Titeux, H., Delvaux, B., 2004. Mobility of radiocesium in three distinct forest floors. Sci. Total Environ. 319, 241–252. https://doi.org/10.1016/S0048-9697(03)00369-3.

Laceby, J.P., Huon, S., Onda, Y., Vaury, V., Evrard, O., 2016. Do forests represent a long-term source of contaminated particulate matter in the Fukushima Prefecture? J. Environ. Manag. 183, 742–753. https://doi.org/10.1016/j.jenvman.2016.09.020.

Lamarque, S., Lucot, E., Badot, P.-M., 2005. Soil-plant transfer of radiocaesium in weakly contaminated forest ecosystems. Radioprotection 40, S407–S412. https://doi.org/10.1051/radiopro:2005s1-060.

Legout, A., Hansson, K., van der Heijden, G., Laclau, J.-P., Mareschal, L., Nys, C., Nicolas, M., Saint-André, L., Ranger, J., 2020. Chemical fertility of forest ecosystems. Part 2: towards redefining the concept by untangling the role of the different components of biogeochemical cycling. For. Ecol. Manag. 461, 117844 https://doi.org/10.1016/j.foreco.2019.117844.

Loffredo, N., Onda, Y., Hurtevent, P., Coppin, F., 2015. Equation to predict the ^{137}Cs leaching dynamic from evergreen canopies after a radio-cesium deposit. J. Environ. Radioact. 147, 100–107. https://doi.org/10.1016/j.jenvrad.2015.05.018, 2015.

Lwila, A.S., Post-Leon, A., Ammer, C., Mund, M., 2023. Site properties, species identity, and species mixture affect fine root production, mortality, and turnover rate in pure and mixed forests of European Beech, Norway spruce, and Douglas-fir. Ecol. Indicat. 147, 109975 https://doi.org/10.1016/j.ecolind.2023.109975.

Mamikhin, S.V., Klyashtorin, A.L., 2000. Mathematical model of ^{137}Cs dynamics in the deciduous forest. J. Environ. Radioact. 47, 101–114. https://doi.org/10.1016/S0265-931X(99)00025-9.

Marques, R., Ranger, J., Villette, S., Granier, A., 1997. Nutrient dynamics in a chronosequence of douglas-fir (Pseudotsuga menziesii (mirb). Franco) stands on the Beaujolais Mounts (France). 2. Quantitative approach. For. Ecol. Manag. 92, 167–197. https://doi.org/10.1016/S0378-1127(96)03913-8.

Meerts, P., 2002. Mineral nutrient concentrations in sapwood and heartwood: a literature review. Ann. For. Sci. 59, 713–722. https://doi.org/10.1051/forest:2002059.

Muto, K., Atarashi-Andoh, M., Matsunaga, T., Koarashi, J., 2019. Characterizing vertical migration of ^{137}Cs in organic layer and mineral soil in Japanese forests: four-year observation and model analysis. J. Environ. Radioact. 208–209, 106040 https://doi.org/10.1016/j.jenvrad.2019.106040.

Myttenaere, C., Schell, W.R., Thiry, Y., Sombre, L., Ronneau, C., Schrieck, J., 1993. Modelling of Cs-137 cycling in forests: recent developments and research needed. Sci. Total Environ. 136, 77–91. https://doi.org/10.1016/0048-9697(93)90298-K.

Nakanishi, T., Matsunaga, T., Koarashi, J., Atarashi-Andoh, M., 2014. ^{137}Cs vertical migration in a deciduous forest soil following the Fukushima Dai-ichi Nuclear Power Plant accident. J. Environ. Radioact. 128, 9–14. https://doi.org/10.1016/j.jenvrad.2013.10.019.

Nakao, A., Thiry, Y., Funakawa, S., Kosaki, T., 2008. Characterization of the frayed edge site of micaceous minerals in soil clays influenced by different pedogenetic conditions in Japan and northern Thailand. Soil Sci. Plant Nutr. 54, 479–489. https://doi.org/10.1111/j.1747-0765.2008.00262.x.

Nicolas, M., Zeller, B., Dambrine, E., Bienaimé, S., Ulrich, E., 2006. Etude isotopique du devenir de l'azote des litières dans les sols de six hêtraies du réseau RENECOFOR. Etude Gest. Sols 13 (1), 33–51 in French. https://hal.inrae.fr/hal-02653642.

Nishikiori, T., Watanabe, M., Masami, K., Koshikawa, M.K., Takamatsu, T., Ishii, Y., Ito, S., Takenaka, A., Watanabe, K., Hayashi, S., 2015. Uptake and translocation of radiocesium in cedar leaves following the Fukushima nuclear accident. Sci. Total Environ. 502, 611–616. https://doi.org/10.1016/j.scitotenv.2014.09.063.

Ohashi, S., Kuroda, K., Takano, T., Suzuki, Y., Fujiwara, T., Abe, H., Kagawa, A., Sugiyama, M., Kubojima, Y., Zhang, C., Yamamoto, K., 2017. Temporal trends in ^{137}Cs concentrations in the bark, sapwood, heartwood, and whole wood of four tree species in Japanese forests from 2011 to 2016. J. Environ. Radioact. 178–179, 335–342. https://doi.org/10.1016/j.jenvrad.2017.09.008.

Ohashi, S., Kuroda, K., Fujiwara, T., Takano, T., 2020. Tracing radioactive cesium in stem wood of three Japanese conifer species 3 years after the Fukushima Dai-ichi Nuclear Power Plant accident. J. Wood Sci. 66, 44. https://doi.org/10.1186/s10086-020-01891-2.

Paul, K.I., England, J.R., Roxburgh, S.H., 2022. Carbon dynamics in tree plantings: How changes in woody biomass impact litter and soil carbon. For. Ecol. Manag. 521, 120406 https://doi.org/10.1016/j.foreco.2022.120406.

Peiffer, M., Badeau, V., Bréda, N., Ulrich, E., 2008. RENECOFOR - Suivi de la météorologie forestière locale (France et Grand-Duché de Luxembourg) - Bilan de la période 1995-2004. In: ONF (Office National des Forêts) ed., Fontainebleau, France, p. 313. https://doi.org/10.17180/KA11-8611 in French. 978-2-84207-325-1.

Penninckx, V., Glineur, S., Gruber, W., Herbauts, J., Meerts, P., 2001. Radial variations in wood mineral element concentrations: a comparison of beech and pedunculate oak from the Belgian Ardennes. Ann. For. Sci. 58, 253–260. https://doi.org/10.1051/forest:2001124.

Ponette, Q., Ulrich, E., Brêthes, A., Bonneau, M., Lanier, M., 1997. RENECOFOR - Chimie des sols dans les 102 peuplements du réseau : campagne de mesures 1993-95. ONF (Office National des Forêts). Fontainebleau, France, p. 427 in French. ISBN 978-2-84207-100-4.

Ponge, J.-F., 2003. Humus forms in terrestrial ecosystems: a framework to biodiversity. Soil Biol. Biochem. 35, 935–945. https://doi.org/10.1016/S0038-0717(03)00149-4.

Quénard, L., Samouëlian, A., Laroche, B., Cornu, S., 2011. Lessivage as a major process of soil formation: a revisitation of existing data. Geoderma 167–168, 135–147. https://doi.org/10.1016/j.geoderma.2011.07.031.

R Core Team, 2013. R: A Language and Environment for Statistical Computing. R Foundation for Statistical Computing, Vienna, Austria. http://www.R-project.org/.

Ranger, J., Marques, R., Colin-Belgrand, M., Flammang, N., Gelhaye, D., 1995a. The dynamics of biomass and nutrient accumulation in a Douglas-fir (Pseudotsuga menziesii Franco) stand studied using a chronosequence approach. For. Ecol. Manag. 72, 167–183. https://doi.org/10.1016/0378-1127(94)03469-D.

Ranger, J., Colin-Belgrand, M., Nys, C., 1995b. Le cycle biogéochimique des éléments majeurs dans les écosystèmes forestiers. Importance dans le fonctionnement des sols. Etude Gest. Sols 2, 119–134 in French. https://www.afes.fr/wp-content/uploads/2023/04/EGS_2_2_RANGER.pdf.

Rantavaara, A., Vetikko, V., Raitio, H., Aro, L., 2012. Seasonal variation of the ^{137}Cs level and its relationship with potassium and carbon levels in conifer needles. Sci. Total Environ. 441, 194–208. https://doi.org/10.1016/j.scitotenv.2012.09.045.

Renaud, P., Champion, D., Brenot, J., 2007. Les retombées radioactives de l'accident de Tchernobyl sur le territoire français : conséquences environnementales et exposition des personnes. In: TEC & DOC Lavoisier ed., collection Sciences et Techniques, p. 190 in French. ISBN 978-2-7430-1027-0.

Ronneau, C., Sombré, L., Myttenaere, C., Andre, P., Vanhouche, M., Cara, J., 1991. Radiocaesium and potassium behaviour in forest trees. J. Environ. Radioact. 14, 259–268. https://doi.org/10.1016/0265-931X(91)90032-B.

Rühm, W., Yoshida, S., Muramatsu, Y., Steiner, M., Wirth, E., 1999. Distribution patterns for stable 133Cs and their implications with respect to the long-term fate of radioactive 134Cs and 137Cs in a semi-natural ecosystem. J. Environ. Radioact. 45, 253–270. https://doi.org/10.1016/S0265-931X(98)00104-0.

Sakashita, W., Miura, S., Akama, A., Ohashi, S., Ikeda, S., Saitoh, T., Komatsu, M., Shinomiya, Y., Kaneko, S., 2020. Assessment of vertical radiocesium transfer in soil via roots. J. Environ. Radioact. 222, 106369 https://doi.org/10.1016/j.jenvrad.2020.106369.

Salleles, J., 2014. Étude du devenir de l'azote dérivé des litières dans le sol et dans l'arbre sur le moyen terme dans les forêts de hêtres par traçage isotopique et modélisation.

PhD Manuscript For. Université de Lorraine 2014, 220. , in French. https://hal.univ-lorraine.fr/tel-01750790.
Sardans, J., Peñuelas, J., 2015. Potassium: a neglected nutrient in global change. Global Ecol. Biogeogr. 24, 261–275. https://doi.org/10.1111/geb.12259.
Sardans, J., Peñuelas, J., 2021. Potassium control of plant functions: ecological and agricultural implications. Plants 10. https://doi.org/10.3390/plants10020419.
Shcheglov, A.I., Tsvetnova, O.B., Klyashtorin, A.L., 2001. Biogeochemical migration of technogenic radionuclides. In: Tikhomirov, F.A. (Ed.), Forest Ecosystems. Nauka, Moscow, Russia, p. 235. https://doi.org/10.13140/2.1.3659.4244. ISBN 5-02-022568-1.
Shcheglov, A., Tsvetnova, O., Klyashtorin, A., 2014. Biogeochemical cycles of Chernobyl-born radionuclides in the contaminated forest ecosystems. Long-term dynamics of the migration processes. J. Geochem. Explor. 144, 260–266. https://doi.org/10.1016/j.gexplo.2014.05.026.
Smolders, E., Van den Brande, K., Merckx, R., 1997. Concentrations of 137Cs and K in soil solution predict the plant availability of ^{137}Cs in soils. Environ. Sci. Technol. 31, 3432–3438. https://doi.org/10.1021/es970113r.
Sombré, L., Vanhouche, M., de Brouwer, S., Ronneau, C., Lambotte, J.M., Myttenaere, C., 1994. Long-term radiocesium behaviour in spruce and oak forests. Sci. Total Environ. 157, 59–71. https://doi.org/10.1016/0048-9697(94)90565-7.
Sparks, D.L., Huang, P.M., 1985. Physical chemistry of soil potassium (chapter 9). In: Munson, R.D. (Ed.), Potassium in Agriculture, pp. 201–276. https://doi.org/10.2134/1985.potassium.c9. ISBN 978-089-118-0869.
Steinhauser, G., Brandl, A., Johnson, T.E., 2014. Comparison of the Chernobyl and Fukushima nuclear accidents: a review of the environmental impacts. Sci. Total Environ. 470–471, 800–817. https://doi.org/10.1016/j.scitotenv.2013.10.029.
Sweeck, L., Wauters, J., Valcke, E., Cremers, A., 1990. The specific interception potential of soils for radiocesium. In: Desmet, G., Nassimbeni, P., Belli, M. (Eds.), Transfer of Radionuclides in Natural and Semi-natural Environments. Elsevier Science Publishers, Brussels and Luxembourg, pp. 249–258, 1990.
Takahashi, J., Onda, Y., Hihara, D., Kenji Tamura, K., 2018. Six-year monitoring of the vertical distribution of radiocesium in three forest soils after the Fukushima Dai-ichi Nuclear Power Plant accident. J. Environ. Radioact. 192, 172–180. https://doi.org/10.1016/j.jenvrad.2018.06.015.
Teramage, M.T., Carasco, L., Orjollet, D., Coppin, F., 2018. The impact of radiocesium input forms on its extractability in Fukushima forest soils. J. Hazard Mater. 349, 205–214. https://doi.org/10.1016/j.jhazmat.2018.01.047.
Thiry, Y., Garcia-Sanchez, L., Hurtevent, P., 2016. Experimental quantification of radiocesium recycling in a coniferous tree after aerial contamination: field loss dynamics, translocation and final partitioning. J. Environ. Radioact. 161, 42–50. https://doi.org/10.1016/j.jenvrad.2015.12.017.
Thørring, H., Skuterud, L., Steinnes, E., 2012. Distribution and turnover of ^{137}Cs in birch forest ecosystems: influence of precipitation chemistry. J. Environ. Radioact. 110, 69–77. https://doi.org/10.1016/j.jenvrad.2012.02.002.
Tikhomirov, F.A., Shcheglov, A.I., Sidorov, V.P., 1993. Forests and forestry: radiation protection measures with special reference to the Chernobyl accident zone. Sci. Total Environ. 137, 289–305. https://doi.org/10.1016/0048-9697(93)90395-M.
Tikhomirov, F.A., Shcheglov, A.I., 1994. Main investigation results on the forest radioecology in the Kyshtym and Chernobyl accident zones. Sci. Total Environ., Forests and Radioactivity 157, 45–57. https://doi.org/10.1016/0048-9697(94)90564-9.
Tsvetnova, O., Shcheglov, A., Klyashtorin, A., 2018. ^{137}Cs and K annual fluxes in a cropland and forest ecosystems twenty-four years after the Chernobyl accident. J. Environ. Radioact. 195, 79–89. https://doi.org/10.1016/j.jenvrad.2018.09.019.
Vandebroek, L., Van Hees, M., Delvaux, B., Spaargaren, O., Thiry, Y., 2012. Relevance of Radiocaesium Interception Potential (RIP) on a worldwide scale to assess soil vulnerability to ^{137}Cs contamination. J. Environ. Radioact. 104, 87–93. https://doi.org/10.1016/j.jenvrad.2011.09.002.
Varga, B., Leclerc, E., Zagyvai, P., 2009. The role of analogues in radioecology. J. Environ. Radioact. 100, 802–805. https://doi.org/10.1016/j.jenvrad.2008.10.004.
Vinichuk, M., Mandro, Y., Kyaschenko, J., Rosén, K., 2023. Soil fertilisation with 137Cs-contaminated and uncontaminated wood ash as a countermeasure to reduce ^{137}Cs uptake by forest plants. J. Environ. Manag. 336, 117609 https://doi.org/10.1016/j.jenvman.2023.117609.
von Fircks, Y., Rosén, K., Sennerby-Forsse, L., 2002. Uptake and distribution of ^{137}Cs and ^{90}Sr in Salix viminalis plants. J. Environ. Radioact. 63, 1–14. https://doi.org/10.1016/S0265-931X(01)00131-X.
Wauters, J., Elsen, A., Cremers, A., Konoplev, A.V., Bulgakov, A.A., Comans, R.N.J., 1996. Prediction of solid/liquid distribution coefficients of radiocaesium in soils and sediments. Part one: a simplified procedure for the solid phase characterisation. Appl. Geochem. 11, 589–594. https://doi.org/10.1016/0883-2927(96)00027-3.
White, P.J., Broadley, M.R., 2000. Mechanisms of caesium uptake by plants. New Phytol. 147, 241–256. https://doi.org/10.1046/j.1469-8137.2000.00704.x.
Winkelbauer, J., Völkel, J., Leopold, M., Hürkamp, K., Dehos, R., 2012. The vertical distribution of Cs-137 in Bavarian forest soils. Eur. J. For. Res. 131, 1585–1599. https://doi.org/10.1007/s10342-012-0626-5.
Yoschenko, V., Takase, T., Konoplev, A., Nanba, K., Onda, Y., Kivva, S., Zheleznyak, M., Sato, N., Keitoku, K., 2017. Radiocesium distribution and fluxes in the typical Cryptomeria japonica forest at the late stage after the accident at Fukushima Dai-Ichi Nuclear Power Plant. J. Environ. Radioact. 166, 45–55. https://doi.org/10.1016/j.jenvrad.2016.02.017.
Yoschenko, V., Takase, T., Hinton, T.G., Nanba, K., Onda, Y., Konoplev, A., Goto, A., Yokoyama, A., Keitoku, K., 2018. Radioactive and stable cesium isotope distributions and dynamics in Japanese cedar forests. J. Environ. Radioact. 186, 34–44. https://doi.org/10.1016/j.jenvrad.2017.09.026.
Yoschenko, V., Nanba, K., Wada, T., Johnson, T.E., Zhang, J., Workman, D., Nagata, H., 2022. Late phase radiocesium dynamics in Fukushima forests post deposition. J. Environ. Radioact. 251–252, 106947 https://doi.org/10.1016/j.jenvrad.2022.106947.
Yoshida, S., Muramatsu, Y., Dvornik, A.M., Zhuchenko, T.A., Linkov, I., 2004. Equilibrium of radiocesium with stable cesium within the biological cycle of contaminated forest ecosystems. J. Environ. Radioact. 75, 301–313. https://doi.org/10.1016/j.jenvrad.2003.12.008.
Yoshida, S., Watanabe, M., Suzuki, A., 2011. Distribution of radiocesium and stable elements within a pine tree. Radiat. Protect. Dosim. 146, 326–329. https://doi.org/10.1093/rpd/ncr181.
Zhang, D., Hui, D., Luo, Y., Zhou, G., 2008. Rates of litter decomposition in terrestrial ecosystems: global patterns and controlling factors. J. Plant Ecol. 1, 85–93. https://doi.org/10.1093/jpe/rtn002.
Zhu, Y., Smolders, E., 2000. Plant uptake of radiocaesium: a review of mechanisms, regulation and application. J. Exp. Bot. 51, 1635–1645. https://doi.org/10.1093/jexbot/51.351.1635.
Zibold, G., Klemt, E., Konopleva, I., Konoplev, A., 2009. Influence of fertilizing on the ^{137}Cs soil-plant transfer in a spruce forest of Southern Germany. J. Environ. Radioact. 100, 489–496. https://doi.org/10.1016/j.jenvrad.2009.03.011.